e-ISSN:2687-6698

# Turkish Journal of Analytical Chemistry

2019

Volume 1
Issue 1
December 2019

www.turkjac.org

e-ISSN: 2687-6698 https://dergipark.org.tr/tr/pub/turkjac

# Turkish Journal of Analytical Chemistry

## TurkJac

**VOLUME 1**
**ISSUE 1**
**December 2019**

**Publication Type:** Peer-reviewed scientific journal
**Publication Date:** December 11, 2019
**Publication Language:** English
Published two times in a year (June, December)

**Authorship, Originality, and Plagiarism:**The authors accept that the work is completely original and that the works of others have been appropriately cited or quoted in the text with the necessary permissions. The authors should avoid plagiarism. It is recommended that they check the article using appropriate software such as Ithenticate and CrossCheck. The responsibility for this matter rests entirely with the authors. All authors will be notified when the manuscript is submitted. If a change of author is needed, the reason for the change should be indicated. Once the manuscript is accepted, no author changes can be made.

**Aims and Scope**

"Turkish Journal of Analytical Chemistry" publishes original full-text research articles and reviews covering a variety of topics in analytical chemistry. Original research articles may be improved versions of known analytical methods. However, studies involving new and innovative methods are preferred. Topics covered include:

- Analytical materials
- Atomic methods
- Biochemical methods
- Chromatographic methods
- Electrochemical methods
- Environmental analysis
- Food analysis
- Forensic analysis
- Optical methods
- Pharmaceutical analysis
- Plant analysis
- Theoretical calculations
- Nanostructures for analytical purposes
- Chemometric methods

**Etik bilgilendirme**

# Contents

## ***Research Articles***




*Author of correspondence:

doi:
e-ISSN: 2687-6698
Research Article

Turkish Journal of Analytical Chemistry
TurkJAC
www.turkjac.org
2019

# Schiff bases carrying dipicolylamine groups for selective determination of metal ions in aqueous media. A phenanthrene-based fluorescent sensor for $Hg^{2+}$ determination

Abidin Gümrükçüoğlu*, Nurhayat Özbek, Tuğba Ak, Elvan Vanlı, Miraç Ocak, Ümmühan Ocak

Karadeniz Technical University, Faculty of Sciences, Department of Chemistry, 61080, Trabzon, Turkey

## Abstract

Four new dipicolylamine compounds carrying anthracene, naphthalene, pyrene and phenanthrene groups were synthesized, and their ion sensor properties were studied by means of emission spectrometry in ethanol-water mixture (1:1). It was disclosed that among a series of studied anions and cations, only with $Cd^{2+}$, $Zn^{2+}$, $Cu^{2+}$ and $Hg^{2+}$ cations, ligands formed complexes selectively. With spectrofluorimetric measurements, the complexation stoichiometries and the complex stability constants of the formed complexes were determined. A linear range from 0.1 μg $L^{-1}$ to 150.00 μg $L^{-1}$ where the fluorescence intensity of the phenanthrene derivative compound showed a regular decrease with the increase of the $Hg^{2+}$ ion concentration was obtained. The method developed for the determination of $Hg^{2+}$ was applied to tap water samples. In order to eliminate the matrix effect, a modified standard addition method was used. Detection and quantification limits were 9.0 μg $L^{-1}$ and 27.0 μg $L^{-1}$, respectively. The recovery rate was above 94.6%. The precision as relative standard deviation (RSD%) was determined as 2.21 for the intra-day measurements while inter-day precision was 3.31.

**Keywords:** Ion sensor, $Hg^{2+}$ determination, dipicolylamine, fluorescence

## 1. Introduction

The significance of metal ions in daily life is a well-known subject. Some metal ions are known to be essential for the human body; their lack or exceed may cause a diversity of diseases whereas others are completely toxic therefore must be out of the scope of human consumption. For example, the effects of $Zn^{2+}$, $Cu^{2+}$ and $Hg^{2+}$ ions on the nervous system are made a subject of research many times [1-2]. $Hg^{2+}$ ion is one of the most dangerous of those ions. Acceptable concentrations of $Hg^{2+}$ ion are determined by law, especially in water resources. Therefore, the detection and determination of this toxic metal cation in environmental systems are significant.

Generally, metal ions are determined with atomic methods. However, these methods are expensive and they usually require pre-treatment and enrichment processes before determination [3-6]. These processes extend the determination period and are disadvantageous when compared to analytical methods based on molecular absorption [7-9]. Therefore, there is a constant need for faster and more economic methods.

Molecular fluorescence methods are selective and sensitive by their nature and they provide simple and quick measurements. With those advantages, they gather attention as an alternative method for metal determination based on atomic absorption. Therefore, many fluorescent sensors were synthesized and recommended for metal determination lately [10].

It is known from the literature that dipicolylamine (DPA) groups tend to form complexes selectively especially with $Zn^{2+}$, $Cu^{2+}$, $Hg^{2+}$

**Citation**: A. Gümrükçüoğlu, N. Özbek, T. Ak, E. Vanlı, M. Ocak, Ü. Ocak, Schiff bases carrying dipicolylamine groups for selective determination of metal ions in aqueous media. A phenanthrene-based fluorescent sensor for $Hg^{2+}$ determination, Turk J Anal Chem 1, 2019, 1-7.

***Author of correspondence**: e-mail: gumrukcuoglu_61@hotmail.com
Tel: +90 462 377 4267, Fax: +90 462 325 3196
Received: October 16, 2019
Accepted: November 06, 2019

ions [11-14]. The metal complexes of the ligands carrying this group were also recommended for the determination of anions with great biological importance such as pyrophosphate and phosphate [15-20]. Moreover, fluorescent DPA ligands were proposed as fluorescent sensors for the determination of metal ions [21-23]. However, there is a lack of reports based on fluorescent DPA ligands to determine metal ions in real samples.

Recently, we have been focusing on the synthesis of new fluorescent DPA ligands in order to determine the effect of the fluorophore group on the ionsensor properties of the Shiff base ligands containing anthracene, naphthalene, phenanthrene, and pyrene groups. We came to the realization that among the ligands presented in these studies, the one carrying the phenanthrene group was allowing the selective and sensitive determination of $Cu^{2+}$ in aqueous media [24]. In the fluoroionophore compounds from the stated study, as donor atoms, oxygen donor atoms were present as an addition to the nitrogen atoms of the DPA group. In the presented study, only nitrogen donor atoms of DPA group are present as cation binders. Our purpose was to disclose the effect of the lack of oxygen donors in their build on similar ion sensor properties of ligands. Thus, four new DPA Schiff base ligands were synthesized and characterized. Among the presented ligands, it has been yet again reported that only the compound carrying the phenanthrene group can be used for the determination of the $Hg^{2+}$ ion in aqueous media, and the proposed spectrofluorimetric method was applied to tap water.

## 2. Experimental

### 2.1. Chemicals

All of the solvents used in the absorption and fluorescence measurements were at spectroscopic purity and purchased from Merck. The 1000 mg $L^{-1}$ standard solvents of all cations and $NO_3^-$, $SO_4^{2-}$ and $PO_4^{3-}$ ions were purchased from Merck and used after proper dilution with deionized water. Sodium salts of ammonium acetate, hydrazine hydrate (%100) and other standard anion solutions were also purchased from Merck (Darmstadt, Germany). Stock solutions of the salts were prepared, then those prepared solutions were diluted and turned into working solutions. All aldehyde compounds were purchased from Sigma-Aldrich (Buch, Switzerland).

### 2.2. Apparatus

For the characterization of new ligands, a FT-IR spectrometer (Perkin Elmer 1600), an NMR spectrometer (Bruker AVANCE III 400 MHz), and an LC-MS spectrometer are used. $^1$H NMR spectra were recorded by $CDCl_3$ with TMS as the internal reference. Deionized water was obtained from a Sartorius Milli-Q system (arium® 611UV). The absorption spectra of the solutions were recorded by Analytic Jena Specord 210 spectrophotometer. A PTI spectrofluorimeter (QM-4/2006) was used for all of the fluorescence measurements.

### 2.3. Measurements

Absorption spectra of the ligands in different solvents containing 10 molar equivalents of $Cu^{2+}$, $Co^{2+}$, $Hg^{2+}$, $Al^{3+}$, $Cr^{3+}$, $Fe^{3+}$, $Pb^{2+}$, $Ni^{2+}$, $Cd^{2+}$, $Zn^{2+}$, $Mn^{2+}$, $Ag^{+}$, $Ba^{2+}$, $Ca^{2+}$, $Mg^{2+}$, $I^-$, $Br^-$, $Cl^-$, $F^-$, $CH_3COO^-$, $NO_3^-$, $CN^-$, $SO_4^{2-}$, $HSO_4^-$, $CO_3^{2-}$, $HCO_3^-$, $PO_4^{3-}$, $P_2O_7^{4-}$ were recorded by using 1-cm absorption cell. Fluorescence spectra under the same conditions were recorded by using a 1-cm quartz cell with a slit width of 1 nm in the range of 380-600 nm. Spectrofluorimetric titration experiments were carried out in the ethanol-water mixture (1:1).

The complex compositions were determined by using the molar ratio graphs from the spectrofluorimetric titrations data. The stability constants were calculated according to the method in the literature [25].

A kind of standard addition method was utilized to determine $Hg^{2+}$ ion in tap water samples. The similar approach has already been reported for $Hg^{2+}$ and $Fe^{3+}$ determination with other fluorescent ligands [26-29]. The proposed method for the determination of $Hg^{2+}$ was applied to the spiked tap water samples.

### 2.4. Synthesis of the ligands

Synthetic pathways for the ligands are given in Scheme 1. Compound **(1)** was synthesized according to the literature [30]. The characterization data of the white solid were consistent with the report in the literature [30].

#### *2.4.1. Synthesis of* ***(3)***

The nitro compound **(3)** was synthesized according to a similar procedure in the literature [24]. The yield of the brown oil product was 86%. IR ($cm^{-1}$): 3051, 3008 (Ar-H), 2928-2822 (C-H), $^1$H-NMR

($CDCl_3$): (δ) 8.49-8.55 (m, 4H, Ar-H), 7.12-7.64 (m, 15H, Ar-H), 3.86 (s, 6H, $CH_2$), 3.98 (s, 6H, $CH_2$).

*2.4.2. Synthesis of* ***(4)***

The amine compound **(4)** was prepared by reduction of the nitro compound **(3)** by using hydrazine hydrate (100%) in n-butanol according to a similar procedure in the literature [24]. The product was obtained as yellow oil (yield, 42%). IR ($cm^{-1}$): 3309-3186 ($NH_2$), 3054-3009 (Ar-H), 2922-2848 (C-H), $^1$H-NMR ($CDCl_3$): (δ) 8.49-8.52 (m, 4H, Ar-H), 7.08-7.60 (m, 15H, Ar-H), 5.88 (s, 2H, $NH_2$), 3.85 (s, 6H, $CH_2$), 3.94 (s, 6H, $CH_2$).

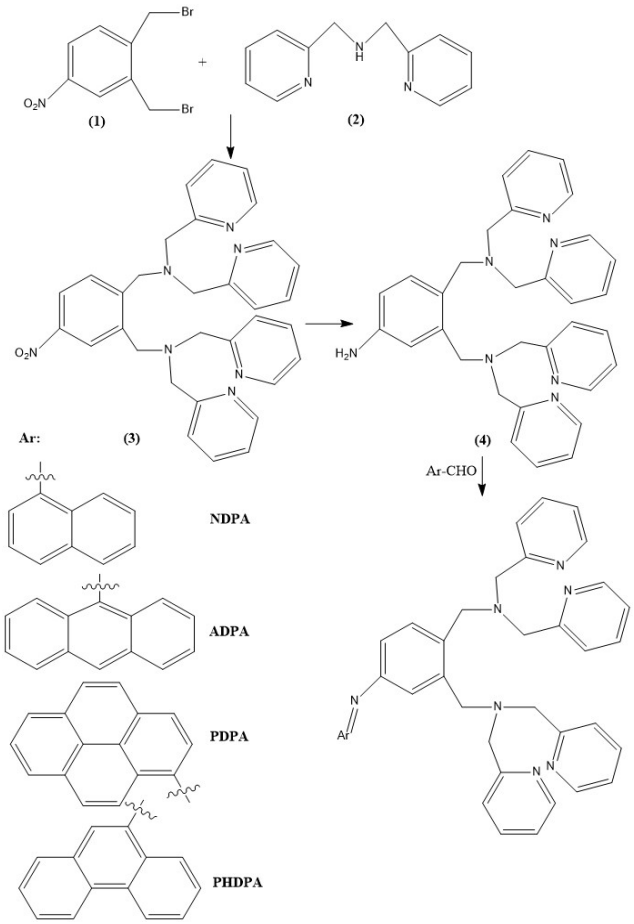


**Scheme 1.** The ligands and their synthetic pathways.

*2.4.3. Synthesis of Schiff bases*

An equivalent amount of aldehyde and amine compound (4) was refluxed in methanol for about 5 hours. The Schiff bases were purified by column chromatography on silica gel using chloroform as an eluent to afford the oil product.

Spectral data: NDPA: Brown oil; IR ($cm^{-1}$): 3050-3008 (Ar-H), 2918-2849 (C-H), 1687 (C=N), $^1$H-NMR ($CDCl_3$): (δ) 9.53 (s, 1H, HC=N), 7.18-9.06 (m, 26H, Ar-H), 3.95 (s, 12H, $CH_2$). ADPA: Brown oil; IR ($cm^{-1}$): 3054-3010 (Ar-H), 2925-2849 (C-H), 1668 (C=N), $^1$H-NMR ($CDCl_3$): (δ) 9.53 (s, 1H, HC=N), 7.18-9.06 (m, 28H, Ar-H), 3.97 (s, 12H, $CH_2$). MS: m/z 701 $[M-2]^+$. PDPA: Brown oil; IR ($cm^{-1}$): 3048-3011 (Ar-H), 2919-2850 (C-H), 1673 (C=N), $^1$H-NMR ($CDCl_3$): (δ) 8.59 (s, 1H, HC=N), 7.22-7.89 (m, 28H, Ar-H), 4.10 (s, 4H, $CH_2$), 4.05 (s, 8H, $CH_2$). PHDPA: Brown oil; IR ($cm^{-1}$): 3055-3008 (Ar-H), 2958-2868 (C-H), 1685 (C=N), $^1$H-NMR ($CDCl_3$): (δ) 8.60 (s, 1H, HC=N), 7.28-8.70 (m, 28H, Ar-H), 3.95 (s, 12H, $CH_2$). MS: m/z 701 $[M-2]^+$.

## 3. Results and discussion

### 3.1. Absorption measurements

The effect of the solvent on the absorption spectra of the ligands was investigated. Many organic solvents were tested as ligand solvent. Ethanol, among the others, gave the highest absorbance values. Therefore, the effect of various ions on the absorption spectra of the ligands was investigated in ethanol: water mixture (1:1). However, with these ions, it was not possible to detect a significant changing in the absorption spectra. Therefore the study was continued with fluorescence measurements.

### 3.2. Emission measurement

Many organic solvents as a ligand solvent were tested to predict the effect of ions on the emission spectra of the ligands. The emission spectra were recorded with excitation wavelength intervals of 10 nm to obtain the maximum emission intensity in different solvents. The ion effects on the emission spectra were remarkable in the case of ethanol between the tested organic solvents as ligand solvent for all ligands. Hence, ethanol was determined as the solvent for the ligands. Eventually, when the solutions containing 10 equivalent ions in ethanol: water mixture (1:1) was investigated, is was proven that no significant chance causing from the tested anions was seen on the ligands' emission spectra (Fig. S1b, Fig. S6b, Fig. S9b, and Fig. S14b). Similar results were obtained for similar dipicolylamine ligands [24].

All the cations investigated caused fluorescence quenching in the emission spectra of ADPA (Fig. S1a). A remarkable quenching was detected especially at the wavelength of 395 and 421 nm. This quenching was the most in the case of $Cu^{2+}$ and $Hg^{2+}$ ions.

Fluorometric titration experiments were made with the cations by using ADPA to monitor the complex formation. The stable complexes were observed with $Cu^{2+}$, $Hg^{2+}$, $Cd^{2+}$ and $Zn^{2+}$ cations. The effect of increasing $Cd^{2+}$ and $Zn^{2+}$ concentration on the emission spectra of ADPA is similar to regular fluorescence enhancements (Fig. S2 and Fig. S3, respectively).

It showed regular emission increase at 418 nm until [M]/[L]=1 during the complexation with $Cd^{2+}$ and after that, a plateau was observed. Hence, the 1:1 complex stoichiometry was detected from the molar ratio graph. The inflection point was 1.0 ([M]/[L]) in the molar ratio graph (Fig. S2 inset above). The similar spectrofluorimetric titration curve was obtained for $Zn^{2+}$ with ADPA (Fig. S3). The complex composition was also 1:1 for this cation (Fig. S3, inset above).

Different from the $Cd^{2+}$ and $Zn^{2+}$ ions, for $Cu^{2+}$and $Hg^{2+}$ ions, fluorescence quenching was obtained at 395, 420 and 442 nm in the spectrofluorimetric titrations with ADPA (Fig. S4 ve Fig. S5). For these cations too, the complex composition was 1:1 (Fig. S4 and S5 insets above).

In the conclusion, even though the spectrofluorimetric titration data disclosed stable 1:1 complexes of ADPA with $Cu^{2+}$, $Hg^{2+}$, $Cd^{2+}$, and $Zn^{2+}$ cations, the results show that the effect of $Cu^{2+}$ and $Hg^{2+}$ on the fluorescence mechanism of the ligand are different from that of $Cd^{2+}$ and $Zn^{2+}$.

All of the fluorescence studies of ADPA were made with other ligands. It is determined that all cations cause quenching in the fluorescence spectra of NDPA (Fig. S6a). The most quenching was determined for $Cu^{2+}$ and $Hg^{2+}$ ions. The studies showed that among the tested cations, only with these ions NDPA formed stable 1:1 complexes (Fig. S7 and Fig. S8, insets above).

Fig. S9a represents the effect of the cations on the fluorescence spectra of PDPA. All cations, unlike ADPA and NDPA, cause an increase in PDPA's fluorescence intensity. The spectrofluorometric titrations showed that only with $Cu^{2+}$, $Hg^{2+}$, $Cd^{2+}$, and $Zn^{2+}$ ions form stable 1:1 complexes with PDPA (Fig. S10, Fig. S11, Fig. S12 and Fig. S13 insets above).

The effect of cations on the fluorescence spectra of PHDPA is shown in Fig. S14a. Similarly to ADPA and NDPA's spectra, all of the cations cause fluorescence quenching. However, only $Hg^{2+}$ ion among the tested cations forms the stable complex with PHDPA as concluded from the fluorescence quenching at 421 nm (Fig. 1 inset above).

To determine the complex stability constants, the ratio of $F_0/(F-F_0)$ or $F_0/(F_0-F)$ was plotted versus 1/[M ] and obtained a good straight line. $F_0$ and F represent the fluorescence intensity of the free ligand solution and the solution containing the ion, respectively. The ratio intercept/slope gives the complex stability constant [25]. The corresponding graphs were given in Fig. S2-5, Fig. S7-8, Fig. S10-13 and, Fig. 1 (inset below).

The stability constants were stated as log K, as seen from Table 1. The most stable complex is ADPA-$Hg^{2+}$ with log K 6.27. The less stable complex was ADPA-$Cd^{2+}$ complex with log K of 4.99.

Table 1 shows that PHDPA compound only forms a stable complex with $Hg^{2+}$ ion among $Cu^{2+}$, $Cd^{2+}$, $Zn^{2+}$ and $Hg^{2+}$ ions, thus it acts as a selective compound for the $Hg^{2+}$ ion. Therefore, the sensor ability of the PHDPA was investigated and detected that it is a suitable ligand to determine $Hg^{2+}$ ion in tap water samples, which has convenient $Hg^{2+}$ content.

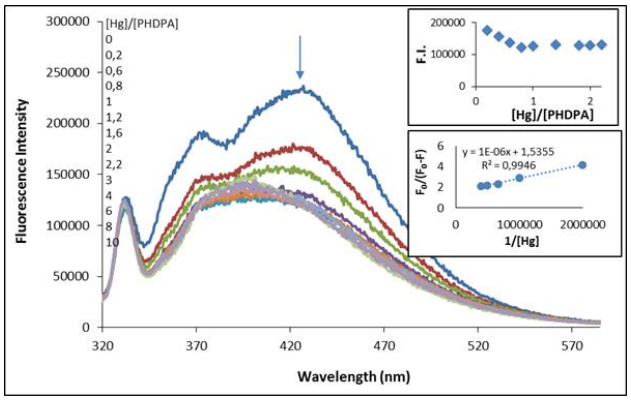


**Figure 1.** The variation of the emission of the ligand (PHDPA) with the concentration of $Hg^{2+}$, added as 0-10 equivalents of $Hg^{2+}$ in ethanol-water mixture (1:1). Ligand concentration= $2.5\times10^{-6}$ M. Excitation at 300 nm. Insets: Measurements were carried out at 421 nm.

### 3.3. Method optimization for $Hg^{2+}$ determination

Non-toxic ethanol was preferred among many tested organic solvents as ligand solvent because it provided high fluorescence intensity. Excitation at 300 nm of PHDPA gave a maximum emission band at 421 nm in ethanol: water mixture (1:1).

Spectrofluorimetric titrations were carried out by using the ligand solutions in the range of $5.0\times10^{-5}$ to $1.0\times10^{-6}$ M with increasing concentrations of $Hg^{2+}$. The values of fluorescence intensity at 421 nm were plotted against $Hg^{2+}$ concentration. The highest $R^2$

value was obtained for a ligand concentration of $2.5\times10^{-6}$ M. Therefore, this concentration was selected for further works.

**Table 1** The complex stability constant values (Log K) in ethanol-water mixture (1:1), (N=3).

| Cation | ADPA | NDPA | PDPA | PHDPA |
|---|---|---|---|---|
| $Cd^{2+}$ | 4.99 ± 0.32 | - | 5.63 ± 0.24 | - |
| $Zn^{2+}$ | 5.72 ± 0.14 | - | 5.05 ± 0.17 | - |
| $Cu^{2+}$ | 5.25 ± 0.22 | 5.74 ± 0.16 | 5.04 ± 0.25 | - |
| $Hg^{2+}$ | 6.27 ± 0.35 | 6.00 ± 0.12 | 5.03 ± 0.28 | 6.18 ± 0.31 |

An external calibration line based on fluorescence quenching of $2.5\times10^{-6}$ M ligand showed linearity within the concentration range from 0.1 μg $L^{-1}$ to 150.00 μg $L^{-1}$. However, recovery was not good in the $Hg^{2+}$ determination in samples using the external calibration graph. Therefore, a modified standard addition method [26-29] was used in the $Hg^{2+}$ determination. The analytical performance data for the proposed method are given in Table 2.

The acceptable recovery results were obtained with the measurements at 421 nm. To optimize the constant $Hg^{2+}$ concentration, various constant $Hg^{2+}$ concentrations (10-50 μg $L^{-1}$) were tested in the modified standard addition method. The optimum constant $Hg^{2+}$ concentration was found at 30.0 μg $L^{-1}$.

**Table 2** Analytical performance data for the $Hg^{2+}$ determination method.

| | |
|---|---|
| Excitation wavelength | 300 nm |
| Emission wavelength | 421 nm |
| LOD | 9.0 μg $L^{-1}$ |
| LOQ | 27.0 μg $L^{-1}$ |
| Linear range | 10-150 (μg $L^{-1}$ - μg $L^{-1}$) |
| Correlation coefficient ($R^2$) | 0.9771 |

### 3.4. The proposed method for $Hg^{2+}$ determination

A kind of standard addition method proposed by our research group was used to determine $Hg^{2+}$ ion [26-29]. In this study, the constant $Hg^{2+}$ concentration and the ligand concentration were 0.03 mg $L^{-1}$ and $2.5\times10^{-6}$ mol $L^{-1}$, respectively. The total volume was 4 mL, the waiting time before the measurement was 1-2 min. Fig. 2 shows the calibration graph for the determination of $Hg^{2+}$ (40.0 μg $L^{-1}$) in the spiked water sample.

### 3.5. Method validation

A linear fluorescence response as a function of $Hg^{2+}$ concentration at 421 nm was obtained in the range of 0.1 μg $L^{-1}$ - 150.00 μg $L^{-1}$. The $R^2$ value was 0.9771 (Fig. 2). The LOD and LOQ values were determined by the standard deviation of eleven measurements of the blank response and the slope of the calibration line according to the IUPAC recommendations. The LOD and LOQ were calculated as $3\times S_d/m$ and $9\times S_d/m$, respectively. $S_d$ was the standard deviation of the blank responses and m was the slope of the calibration line. The LOD and LOQ values were 9.0 μg $L^{-1}$ and 27.0 μg $L^{-1}$, respectively. The accuracy of the proposed method was tested by recovery measurements. A modified standard addition method was applied to tap water samples of KTU campus in Trabzon. The $Hg^{2+}$ concentration of 40.0 μg $L^{-1}$ was provided in three tap water samples in spiking processes. The recovery rate was above 94.6 %. The tap water samples were diluted in various proportions. But the acceptable recovery results in the tap water samples were obtained at 1/4 dilution. Therefore, the tap water samples were diluted in a ratio of 1/4 before spiking to obtain the acceptable recovery results. The results showed that the proposed method can be applied for the determination of mercury in water samples, which has convenient $Hg^{2+}$ content. The intra-day and inter-day precision were estimated by analysing three spiked tap water samples. The precision as relative standard deviation (RSD %) was determined as 2.21 for the intra-day measurements while inter-day precision was 3.31.

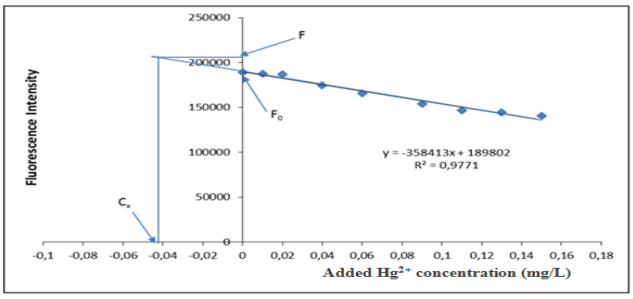


**Figure 2.** Modified standard addition plot to determine $Hg^{2+}$ with PHDPA. Ligand concentration= $2.5\times10^{-6}$ M. Excitation at 300 nm. Measurement was carried out at 421 nm.

### 3.6. Quenching mechanism

The Stern-Volmer relationship [31] was utilized to determine the efficiency of the quenching of a fluorophore by a quencher (Equation 1).

$$F_0 / F = 1 + K_{sv}[Q] \quad (1)$$

In Eq. 1, $K_{sv}$ is the Stern-Volmer quenching constant and [Q] is the concentration of the quencher. $F_0$ and F represent the fluorescence intensity in the absence and the presence of the

quencher, respectively. When the system obeys the Stern-Volmer equation, a plot of $F_0/F$ versus molar concentration of the quencher has given a straight line with a slope of $K_{sv}$ and a y-axis intercept of 1.

Fig. 3 shows the Stern-Volmer analysis based on steady-state emission for the complexation of $Hg^{2+}$ by PHDPA. $F_0/F$ term linearly increased with increasing $Hg^{2+}$ concentration until 40.0 μg $L^{-1}$. As seen in Fig. 3, y-axis intercept is about 1. The Stern-Volmer relationship is obtained in the case of both dynamic and static quenching [31]. It is well known, static quenching results from the formation of the ground state complex [31]. In this study, the 1:1 complex formation with $Hg^{2+}$ was determined. Therefore, it is concluded that the observed quenching should be a static quenching.

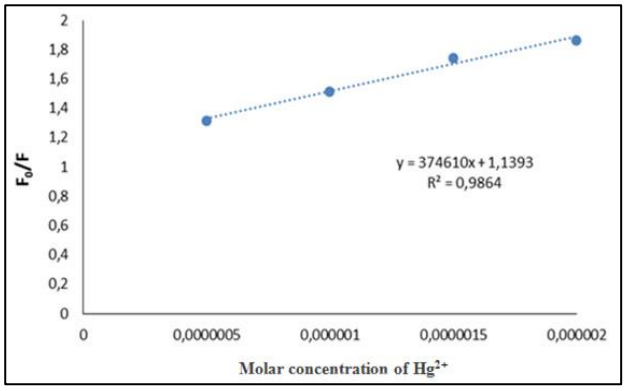


**Figure 3.** Stern-Volmer plot for the quenching of **PHDPA** by $Hg^{2+}$.

## 4. Conclusions

New fluorescent Schiff base ligands carrying dipicolylamine groups were synthesized from the aldehyde compounds having pyrene, naphthalene, anthracene, and phenanthrene groups. The fluorescent Schiff base carrying phenanthrene group PHDPA showed selectivity for $Hg^{2+}$ ion among many metal ions. Therefore, it was used to develop a new $Hg^{2+}$ determination method in aqueous media. To show the accuracy of the proposed method, the spiked tap water samples were analyzed. Recovery values were acceptable. These results suggest that the new Schiff base carrying phenanthrene group (PHDPA) can be used as an analytical ligand for the determination of $Hg^{2+}$ in water samples. The proposed method is relatively economical, time-saving and simpler with respect to convenient atomic methods.

## Acknowledgments

The Scientific and Technological Research Council of Turkey (TUBITAK) supported this work (project no: 114Z387).

## References

[1] L.M. Plum, L. Rink, H. Hajo, The essential toxin: Impact of zinc on human health, Int J Environ Res Public Health, 7(4), 2010, 1342-1365.

[2] B. Fernandes Azevedo, L. Barros Furieri, F.M. Peçanha, G.A. Wiggers, P. Frizera Vassallo, M. Ronacher Simões, J. Fiorim, P. Rossi de Batista, M. Fioresi, L. Rossoni, Toxic effects of mercury on the cardiovascular and central nervous systems, J Biomed Biotechnol, 2012, DOI: 10.1155/2012/949048.

[3] H. Refiker, M. Merdivan, R.S. Aygun, Selective preconcentration of gold from ore samples, Int J Anal Chem., 2018, 7503202.

[4] M.R. Ganjali, L.H Babaei, A. Badiei, K. Saberian, S. Behbahani, G. M. Ziarani, M. Salavati- Niasari, A novel method for fast enrichment and monitoring of hexavalent and trivalent chromium at the ppt level with modified silica MCM-41 and its determination by inductively coupled plasma optical emission spectrometry, Química Nova, 29(3), 2006, 440-443.

[5] K. Pyrzynska, T. Wierzbicki, Solid-phase extraction for preconcentration and separation of vanadium species in natural waters, Microchim Acta, 147(1-2), 2004, 59-64.

[6] I.L. Alcantara, P.S. Roldan, G.R Castro, F.V. Moraes, F.A. Silva, C.C. Padilha, J.D. Oliveira, P.M. Padilha, Determination of cadmium in river water samples by flame aas after on-line preconcentration in mini-column packed with 2-aminothiazole-modified silica gel, Anal Sci, 20(7), 2004, 1029-1032.

[7] V.A. Lemos, L.O. Dos Santos, A new method for preconcentration and determination of mercury in fish, shellfish and saliva by cold vapour atomic absorption spectrometry, Food Chem, 149, 2014, 203-207.

[8] M. Ali, Preconcentration and determination of trace amounts of heavy metals in water samples using membrane disk and flame atomic absorption spectrometry, Chinese J Chem, 25(5), 2007, 640-644.

[9] N. Altunay, R. Gürkan, A simple and efficient approach for preconcentration of some heavy metals in cosmetic products before their determinations by flame atomic absorption spectrometry, Turk J Chem, 40, 2016, 988-1001.

[10] B. Valeur, I. Leray, Design principles of fluorescent molecular sensors for cation recognition, Coord Chem Rev, 205(1), 2000, 3-40.

[11] L.G. Pathberiya, N. Barlow, T. Nguyen, B. Graham, K.L. Tuck, Facile, divergent route to bis-Zn(II) dipicolylamine type chemosensors for pyrophosphate, Tetrahedron, 68(46), 2012, 9435-9439.

[12] J.H. Kim, J.Y. Noh, I.H. Hwang, J. Kang, J. Kim, C. Kim, An anthracene-based fluorescent chemosensor for $Zn^{2+}$, Tetrahedron Lett, 54(19), 2013, 2415-2418.

[13] A. Coskun, M. Deniz Yilmaz, E.U. Akkaya, An acenaphthopyrrolone-dipicolylamine derivative as a selective and sensitive chemosensor for group IIB cations, Tetrahedron Lett, 47(22), 2006, 3689-3691.

[14] H. Lee, R.D. Hancock, H.S. Lee, Role of fluorophore–metal interaction in photoinduced electron transfer (pet) sensors: time-dependent density functional theory (TDDFT) study, J Phys Chem A, 117(50), 2013, 13345-13355.
[15] A. Ojida, Y. Mito-Oka, M.A. Inoue, I. Hamachi, First artificial receptors and chemosensors toward phosphorylated peptide in aqueous solution, J Am Chem Soc, 124(22), 2002, 6256-6255.
[16] K.H. Chen, J.S. Yang, C.Y. Hwang, J.M. Fang, Phospholipid-induced aggregation and anthracene excimer formation, Org Lett, 10(20), 2008, 4401-4404.
[17] T. Sakamoto, A. Ojida, I. Hamachi, Molecular recognition, fluorescence sensing, and biological assay of phosphate anion derivatives using artificial Zn(II)–Dpa complexes, Chem Commun (Camb), (2), 2009, 141-152.
[18] J.F. Zhang, S. Kim, J.H. Han, S.J. Lee, T. Pradhan, Q.Y. Cao, S.J. Lee, C. Kang, J.S. Kim, Pyrophosphate-selective fluorescent chemosensor based on 1,8-naphthalimide–dpa–zn(ii) complex and its application for cell imaging, Org Lett, 13(19), 2011, 5294-5297.
[19] S. Watanabe, K. Ohtsuka, S. Sato, S. Takenaka, Discrimination of phosphorylated double stranded DNA by naphthalene diimide having zinc(II) dipicolylamine complexes, Bioorganic Med Chem, 19(3), 2011, 1361-1365.
[20] M.J. Kim, K.M.K. Swamy, K.M. Lee, A.R. Jagdale, Y. Kim, S.-J. Kim, K.H. Yoo, J. Yoon, Pyrophosphate selective fluorescent chemosensors based on coumarin–DPA–Cu(II) complexes, Chem Commun (Camb), (46), 2009, 7215-7217.
[21] J. Hatai, S. Bandyopadhyay, Altered selectivity of a dipicolylamine based metal ion receptor, Chem Commun (Camb), (50), 2014, 64-66.
[22] S.K. Lee, M.G. Choi, J. Choi, S.K. Chang, Fluorescence signaling of $Zn^{2+}$ levels in synthetic urine by dipicolylamine-armed hydroxynaphthalimide, Sensors Actuators, B Chem, 207, 2015, 303-307.
[23] K. Komatsu, Y. Urano, H. Kojima, T. Nagano, Development of an iminocoumarin-based zinc sensor suitable for ratiometric fluorescence imaging of neuronal zinc, J Am Chem Soc, 129(44), 2007, 13447-13454
[24] E. Vanlı, M.N. Mısır, H. Alp, T. Ak, N. Özbek, Ü. Ocak, M. Ocak, Ion sensor properties of fluorescent schiff bases carrying dipicolylamine groups a simple spectrofluorimetric method to determine Cu(II) in water samples, J. Fluoresc., 27(5), 2017, 1759-1766.
[25] J. Bourson, B. Valeur, Ion-responsive fluorescent compounds. 2. Cation-steered intramolecular charge transfer in a crowned merocyanine, J Phys Chem, 93(9), 1989, 3871-3876.
[26] A. Başoğlu, G. Tosun, M. Ocak, H. Alp, N. Yaylı, Ü. Ocak, Simple time-saving method for iron determination based on fluorescence quenching of an azaflavanon-3-ol compound, J Agric Food Chem, 63(10), 2015, 2654-2659.
[27] Y. Çağlar, E.T. Saka, H. Alp, H. Kantekin, Ü. Ocak, M. Ocak, A simple spectrofluorimetric method based on quenching of a nickel(II)-phthalocyanine complex to determine iron (III), J Fluoresc, 26(4), 2016, 1381-1389.
[28] M. Ocak, T. Ak, A. Aktaş, N. Özbek, O.C. Çağılcı, A. Gümrükçüoğlu, H. Kantekin, Ü. Ocak, H. Alp, Metal complexation properties of Schiff bases containing 1,3,5-triazine derived from 2-hydroxy-1-naphthaldehyde in solution. A simple spectrofluorimetric method to determine mercury (II), J Fluoresc, 27(1), 2017, 59-68.
[29] N. Özbek, H. Alp, G. Çelik, T. Ak, O.C. Çağılcı, N. Yaylı, Ü. Ocak, M. Ocak. A simple spectrofluorimetric method for iron determination with a chalcone-based schiff base, J Fluoresc, 27(2), 2017, 635-641.
[30] M.P. Hay, K.O. Hicks, K. Pchalek, H.H. Lee, A. Blaser, F.B. Pruijn, R.F Anderson, S.S. Shinde, W.R. Wilson, W.A. Denny, Tricyclic [1,2,4] triazine 1,4-dioxides as hypoxia selective cytotoxins, J Med Chem, 51(21), 2008, 6853-6865.
[31] J.R. Lakowicz, Principles of fluorescence spectroscopy, Kluwer, New York, 1999.

doi:
e-ISSN: 2687-6698
Research Article
Turkish Journal of Analytical Chemistry
TurkJAC
www.turkjac.org
2019

# Schiff base derivatives with morpholine and antioxidant activity

Dilek Ünlüer[1]*, Ersan Bektaş[2], Yasemin Ünver[1]

[1]Karadeniz Technical University, Faculty of Science, Department of Chemistry, 61080, Trabzon, Turkey

[2]Giresun University, Espiye Vocational School, Department of Property Protection and Security, 28600, Espiye, Giresun, Turkey

## Abstract

New Schiff base derivatives with morpholines, 4-bromo-2-(((4-morpholinophenyl)imino)methyl)phenol (**I**) and 4-bromo-2-(((2-morpholinoethyl) imino) methyl)phenol (**II**) were synthesized. The compounds **I**- **II** were characterized by spectral methods IR, and NMR spectroscopic techniques. Antioxidant activities of compounds **I** and **II** were determined by the ferric reducing ability of plasma (FRAP) assay method which is based on the reduction of $Fe^{3+}$ -TPTZ complex to the $Fe^{2+}$ -TPTZ complex in the presence of antioxidants and 2,2-diphenyl-1-picrylhydrazyl (DPPH) assay methods. It was concluded that the compounds **I** and **II** had no radical scavenging activity. In the FRAP assay, higher $FeSO_4.7H_2O$ equivalent, indicating stronger antioxidant activity. Accordingly, it has been found that compound **I** has relatively high ferric reducing power ability (i.e., antioxidant activity) than compound **II**. The ability of compounds **I** and **II** to reduce iron (III) to iron (II) ions were calculated as 929 and 11 μM $FeSO_4.7H_2O$ equivalent/g sample, respectively. To summarize, the above-mentioned results indicate that compound **II** has inefficient ferric reducing activity and compound **I** has effective ferric reducing activity.

**Keywords:** Schiff base, morpholine, antioxidant activity, IR and NMR spectroscopy, FRAP, DPPH

## 1. Introduction

Antioxidants are very essential chemical substances for the human body. These substances can be produced by human body cells on their own and can be obtained through some nutrients. Antioxidants are effective protection against all diseases the use of antioxidants is intensively studied in medicinal chemistry, especially as a means for the treatment of these widespread diseases such as Parkinson, Alzheimer, heart failure and cancer, that may disturb human health.

It is also observed by experts that the antioxidant retards symptoms such as aging. Therefore, synthetic compounds are mostly studied for their antioxidant activities by using different methods [1-2]. Schiff bases which are including azomethine functional group (N=CH) possess a broad spectrum of biological activities such as antipyretic, cytotoxic, antimalarial, antipyretic, antimycobacterial, antimicrobial, anticancer, antioxidant, anti-inflammatory, antiviral, and DNA cleavage properties [3-7].

Schiff base derivatives are used in optoelectronic applications as the most important class of photochromic materials [6]. The metal complexes of Schiff bases are important compounds in inorganic chemistry for biological applications in clinical and pharmacological areas [8-10].

Morpholines have pharmacological activities such as antiemetic, antimicrobial, proteinemic, antihyperlipo, platelet aggregation inhibitory, anticancer, antiemetic, antihyperlipo, antiproliferative, and bronchodilator activity [11].

Due to their significant biological properties, Schiff base derivatives with morpholine, 4-bromo-2-(((4-morpholinophenyl)imino)methyl)phenol (**I**) and 4-bromo-2-(((2-morpholinoethyl)imino)methyl)-phenol (**II**), were synthesized and characterized by IR and NMR spectroscopic methods in this study.

**Citation**: D.Ünlüer, E. Bektaş, Y. Ünver, Schiff base derivatives with morpholine and antioxidant activity, Turk J Anal Chem, 1, 2019, 8-10.

***Author of correspondence:** e-mail: dunluer@yahoo.com
Tel: +90 546 477 5361, Fax: +90 462 3253196
Received: November 04, 2019
Accepted: November 18, 2019

The total antioxidant capacities of **I** and **II** were analyzed by FRAP method, which is based on the reduction of $Fe^{3+}$-TPTZ complex to the $Fe^{2+}$-TPTZ complex in the presence of antioxidants and 2,2-diphenyl-1-picrylhydrazyl (DPPH) assay methods.

## 2. Experimental

### 2.1. Chemistry

A Varian-Mercury 400 MHz spectrometer was utilized to record the $^1$H-NMR and $^{13}$C-NMR spectra. TMS and DMSO-$d_6$ were utilized as an internal standard and solvent, respectively. A Perkin-Elmer FT-IR spectrometer was used to obtain IR spectra preparing KBr pellets. An electrothermal apparatus was used to determine melting points and were not verified.

### 2.2. Synthesis of compound II

5-bromo-2-hydroxybenzaldehyde (0.01 mol) and 2-morpholinoethan (0.01 mol) were stirred for 1 h. at 180-200 °C in the oil bath. The reaction was monitored by thin-layer chromatography (TLC). The reaction content cooled to room temperature. The obtained solid was recrystallized from a mixture of DMSO and water. The synthesis of compounds I-II is presented in Scheme 1.

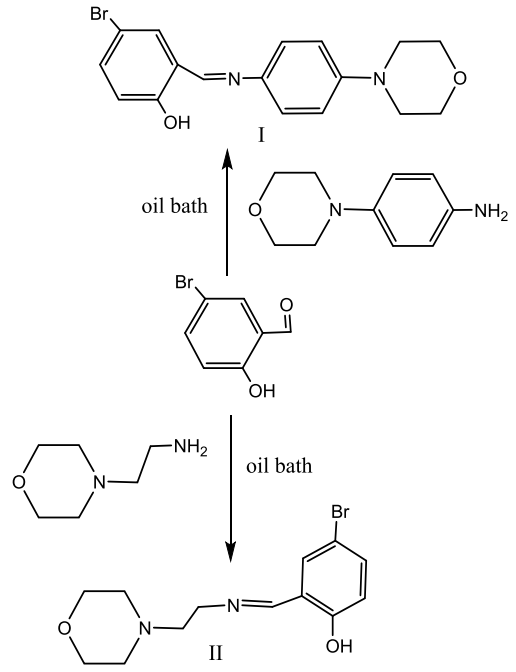


**Scheme 1.** Synthesis pathways of compounds I-II.

4-bromo-2-(((4-morpholinophenyl)imino)methyl) -phenol (**I**) was published in literature [12].

4-bromo-2-(((2-morpholinoethyl)-imino)methyl)-phenol (**II**)**:** Yield: 83.08 %; m.p. 252-253 °C; IR (ν, $cm^{-1}$): 2966 (CH), 1633 (C=N), 1605 (C=C); $^1$H-NMR (δ ppm): 2.42 (4H, t, morpholine N-$CH_2$), 2.60 (2H, t, N-$CH_2$-$CH_2$), 3.56 (4H, t, morpholine O-$CH_2$), 3.70 (2H, t, $CH_2$-N=CH), 6.85 (1H, d, Arom. H), 7.44-7.46 (1H, m, Arom. H), 7.65 (1H, d, Arom. H), 8.53 (1H, s, NH), 13.77 (1H, s, OH); $^{13}$C-NMR (δ ppm): 52.66 (morpholine N-$CH_2$), 54.08 ($CH_2$-N=CH), 57.60 (N-$CH_2$-$CH_2$), 65.58 (morpholine O-$CH_2$), 108.02 (Arom. C), 118.77 (Arom. CH), 119.47 (Arom. C), 1132.83 (Arom. CH), 134.22 (Arom. CH), 160.31 (Arom. C), 164.65 (HC=N).

### 2.3. Determination of Antioxidant Activity

The antioxidant activities of the compounds **I** and **II** were analyzed by two commonly preferred methods (FRAP and DPPH tests), which are considered as a good indicator of the antioxidant capability of various compounds.

The radical scavenging effects of the compounds **I** and **II** against the 2,2-diphenyl-1-picrylhydrazyl (DPPH) radical were examined according to the method of Molyneux [11] with some alterations. In the presence of an antioxidant, it is based on the decolorization of the purple color of DPPH, and the change in absorbance is measured spectrophotometrically at 517 nm. A volume of 0.75 mL of 0.1 mM DPPH in methanol was mixed with an equal volume of dissolved compound solution in DMSO (at various concentrations), shaken well, kept in the dark for 50 minutes, and activity measured at 517 nm using Trolox as standard and values were revealed as $SC_{50}$ (μg sample per mL).

The antioxidant capacities of compounds **I** and **II** were also analyzed by FRAP method, which is based on the reduction of $Fe^{3+}$ -TPTZ complex to the $Fe^{2+}$ -TPTZ complex in the presence of antioxidants [12]. 3 ml of freshly prepared FRAP reagent (containing TPTZ, $FeCl_3$, and acetate buffer pH: 3.6) and 100 μl of the stock solutions of compounds **I** and **II** or the blank (DMSO) were mixed in the test tube. Subsequently, absorbance values were determined at 593nm after 4 minutes of incubation at 37 °C. FRAP solution as a reagent and sample blanks were also investigated. The sum of the two measurements was subtracted to obtain the final absorbance. The last absorbance was compared with the $FeSO_4.7H_2O$ standard curve (31.25-1000 μM). The results were given as μM$FeSO_4.7H_2O$ equivalent per gram of compound. Higher $FeSO_4.7H_2O$ equivalent values

indicate higher FRAP values and this means higher antioxidant capacity.

## 3. Results and discussion

### 3.1. Chemistry

In the IR spectrum of compound **II**, while $NH_2$ signals belonging to starting aldehyde compound disappeared, the vibration of C=N group occurred at 1633 $cm^{-1}$. In the $^1H$ NMR spectrum of the compound **II**, proton signal belonging to N=CH was observed at 8.53 ppm as a singlet. In addition, N=CH carbon signal occurred at 164.65 ppm in the $^{13}C$-NMR spectrum. Furthermore, the other NMR data also supported the structure of compound **II**.

### 3.2. Antioxidant Activities

In this study, FRAP and DPPH tests were implemented to calculate the antioxidant activities of compounds **I** and **II** and the results are given in Figure 1. In the DPPH test, antioxidant activities could not be determined due to the turbidity of the substances in all replicates. Therefore, it was concluded that these substances had no radical scavenging activity.

In the FRAP assay, higher $FeSO_4.7H_2O$ equivalent, indicating stronger antioxidant activity. Accordingly, it has been found that compound **I** has relatively high ferric reducing power ability (i.e., antioxidant activity) than compound **II**. The ability of compounds **I** and **II** to reduce iron (III) to iron (II) ions were calculated as 929 and 11 μM $FeSO_4.7H_2O$ equivalent/g sample, respectively. To summarize, the above-mentioned results indicate that compound **II** has inefficient ferric reducing activity and compound **I** has effective ferric reducing activity.

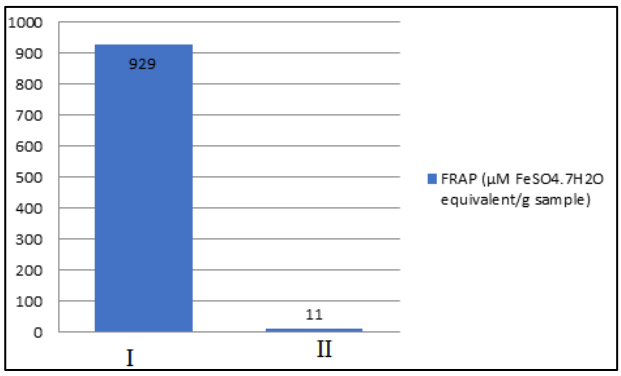


**Figure 1.** Ferric reducing antioxidant power (FRAP) of compounds (I-II).

## References

[1] Z. Liu, B. Wang, Z. Yang, Y. Li, D. Qin, T. Li, Synthesis, crystal structure, DNA interaction and antioxidant activities of two novel water-soluble Cu(2+) complexes derivated from 2-oxo-quinoline-3-carbaldehyde Schiff-bases, Eur J Med Chem 44, 2019, 4477-4484.

[2] H. Hussain, G. Babic, T. Durst, J. Wright, M. Flueraru, A. Chichirau, L.L. Chepelev, Development of novel antioxidants: Design, synthesis, and reactivity, Org Chem 6, 2013, 7023-7032.

[3] Y. Ünver, K. Sancak, F. Çelik, E. Birinci, M. Küçük, S. Soylu, N.A. Burnaz, New thiophene-1,2,4-triazole-5(3)-ones: Highly bioactive thiosemicarbazides, structures of schiff bases and triazole-thiols, Eur J Med Chem 84, 2014, 639-650.

[4] Y. Ünver, S. Deniz, F. Çelik, Z. Akar, M. Küçük, K. Sancak, Synthesis of new 1,2,4-triazole compounds containing Schiff and Mannich bases (morpholine) with antioxidant and antimicrobial activitie, J Enzyme Inhib Med Chem 31(3S), 2016, 89-95.

[5] Y. Ünver, E. Bektaş, Synthesis and biological activity of new Schiff bases of benzylideneamine bearing thiophene, 1,2,4-triazolone, 1,3,4-oxadiazole, morpholine moieties, Lett Drug Des Discov 15, 2018, 706-712.

[6] Y. Ünver, E. Bektaş, Ş. Direkel, Synthesis and antioxidant and antileishmanial activities of new bis n-amino triazole derivatives, Russ J Gen Chem 88, 2018, 2616-2620.

[7] Y. Ünver, M. Tuluk, N. Kahriman, E. Emirik, E. Bektaş, Ş. Direkel, New chalcone derivatives with schiff base-thiophene: synthesis, biological activity and molecular docking studies, Russ J Gen Chem 89, 2019,794-799.

[8] Y. Ünver, H. Baş, Z. Bıyıklıoğlu, Non-peripherally 4-{[(1E)-1-benzothien-2-ylmethylene]amino}phenol substituted zinc(II), manganese(III), cobalt(II) phthalocyanines: Synthesis and electrochemistry, J Mol Struct 1178, 2019, 508-513.

[9] K. Serbest, A. Özen, Y. Ünver, M. Er, İ. Değirmencioğlu, K. Sancak, Spectroscopic and theoretical study of 1,2,4-triazole-3-one based salicylaldimine complexes and evaluation of superoxide-scavenging properties, J Mol Struct 922, 2009, 1-10.

[10] K. Serbest, İ. Değirmencioğlu, Y. Ünver, M. Er, C. Kantar, K. Sancak, Microwave-assisted synthesis and characterization and theorical calculations of the first example of free and metalo phthalocyanines from salen type Schiff base derivative bearing thiophen and triazole heterocyclic ring, J Organomet Chem 692, 2007, 5646-5654.

[11] P. Molyneux, The use of the stable free radical diphenylpicryl-hydrazyl (DPPH) for estimating antioxidant activity, Songklanakarin J Sci Technol, 2004, 26(2), 211-219.

[12] I.F.F. Benzie, Y.T. Szeto, Total antioxidant capacity of teas by the ferric reducing/antioxidant power assay, J Agric Food Chem 47(2), 1999, 633-636.

doi:
e-ISSN: 2687-6698
Research Article
Turkish Journal of Analytical Chemistry
www.turkjac.org
2019
TurkJAC

# Production of propolis/$TiO_2$ (P-$TiO_2$) nano composites for degradation of food dyes

Melek Koç Keşir[1], Münevver Sökmen[2]*

[1]Karadeniz Technical University, Faculty of Science, Department of Chemistry, 61080, Trabzon, Turkey

[2]Konya Food and Agriculture University, Faculty of Engineering and Architecture, Department of Bioengineering, 42080, Konya, Turkey

## Abstract

The aim of this study is to produce highly active hybrid propolis-$TiO_2$ nanocomposites using the sol-gel method and to use it in remediation of food industry waste. Propolis solution was prepared in ethanol and added to the sol-gel mixture at increasing volume (0.25, 0.50, 0.75, 1.00 mL) to prepare propolis-$TiO_2$ (P-$TiO_2$) hybrid catalyst. Neat $TiO_2$ was also prepared by the same sol-gel technique and its action was compared to propolis doped ones. Catalysts were calcinated at 300°C to obtain the desired anatase form. After production the catalysts were characterized by X-ray diffraction (XRD), scanning electron microscopy (SEM) and FTIR. Sunset Yellow (SY), Allura red (AR) and Tartrazine (TT) were used as model compounds ($[C]_0$=10 mg $L^{-1}$, catalyst mass=1 g $L^{-1}$). The concentration of dyes was monitored by UV-vis spectrometry. P-$TiO_2$ catalyst prepared with 1.00 mL propolis solution was extremely effective for removal of all dyes studies for both 254 nm and 365 nm light exposure. LED light exposure provided lower removal rate (approx. 25%) but it was still significant for dye removal.

**Keywords:** Photocatalysis, propolis-$TiO_2$, food dye

## 1. Introduction

$TiO_2$ is a well-known photocatalyst and surface modification is done to obtain more effective nanoparticles. The modification can be accomplished by either direct wet deposition or sol-gel methods. Sol-gel methods have some advantages due to controllable stoichiometry and homogenous dispersion of both dopant and $TiO_2$. The main photocatalytic material is usually $TiO_2$ and dopants are immobilized on its surface or its inner layers. $TiO_2$ shows relatively high reactivity (anatase crystalline phase) and chemical stability under ultraviolet light is lower than 387 nm. There are many doping materials to develop photocatalysts exhibiting high reactivity under visible light ($\lambda$>400 nm). Visible light-activated $TiO_2$ could be prepared by metal-ion implantation, metal or non-metal immobilization, dye sensitization [1,2]. On the contrary, $TiO_2$ was immobilized on several support matrices such as silica, zeolite, clay, and activated carbons [3].

Doping of $TiO_2$ with the compounds such as activated carbon adds some superior properties such as increased adsorption capacity, higher surface area, robust and stable structures and compositions [4]. Additionally, carbon doping can significantly stabilize the anatase $TiO_2$ and improve the adsorption of organic pollutant molecules on the catalyst surface as well as shifting its absorption band to longer wavelength. Carbonaceous doping promotes the interaction and facilitates the interphase transfer of the target compounds to the $TiO_2$ phase. Some studies have been reported for the C-doping of $TiO_2$ [4,5]. Propolis immobilized $TiO_2$ hybrid nanocomposites might be a good choice for the removal of food dye effluents. A proper immobilization of this biocompatible material on

**Citation:** M. Koç Keşir, M. Sökmen, Production of propolis/$TiO_2$ (P-$TiO_2$) nano composites for degradation of food dyes, Turk J Anal Chem, 1, 2019, 11-16.

***Author of correspondence**: e-mail: munevver.sokmen@gidatarim.edu.tr
Tel: +90 332 2235451, Fax: +90 332 2235490
Received: November 06, 2019
Accepted: November 18, 2019

photocatalyst is a new approach in photocatalytic studies. Especially sol-gel production might be a good alternative to produce propolis-$TiO_2$ nanostructures (P-$TiO_2$) to increase the effectiveness of this valuable photocatalyst. The aim of this study is to produce highly active hybrid propolis-$TiO_2$ nanocomposites using the sol-gel method and to use its remediation of food industry waste. After the production of the catalyst P-$TiO_2$ hybrid catalysts were characterized by X-ray diffraction (XRD), scanning electron microscopy (SEM) and FTIR. In the current literature, there are a few reported studies related to photocatalytic removal of food colouring dye effluents. Photocatalytic Tartrazine degradation using ZnO as photocatalyst has been reported by Rahman et al. [6]. Another work was published by Zazouli et al. [7] for photocatalytic removal of food dye Brilliant Blue FCF using $Fe_3O_4$-$TiO_2$ hybrid catalyst. The catalyst was effective and degraded the dye using UVC and LED (Light Emitting Diodes) light. In the present study Sunset Yellow (SY), Allura red (AR) and Tartrazine (TT) were used as model compounds (Figure 1). The concentration of dyes was monitored by UV-vis spectrometry before and after treatment. Dye removal percentages were calculated from the remaining dye concentration after a certain treatment period.

## 2. Experimental

### 2.1. Materials and reagents

Propolis is a resinous natural substance that is produced by bees to protect the hive against external threats such as bacteria and viruses. Raw propolis sample was collected from local bee producers in the 2018 season (Trabzon, Turkey) and was stored at +4°C. Propolis samples (each 5 g) were weighed and added to 100 mL of methanol. The samples were continuously stirred with a shaker at room temperature for 24 h before the suspension was centrifuged at 10,000 G for 15 min. The supernatant was concentrated in a rotary evaporator under reduced pressure at 40°C. Then, the residue resolved in a minimal volume of 98% absolute ethanol. The ethanolic extract was directly used in the sol-gel process. All chemicals were analytical grade and purchased from Sigma-Aldrich. The chemical structures of dye molecules are given in Figure 1. Dye solutions were prepared in deionized at 10 mg $L^{-1}$ concentration.

### 2.2. Sol-Gel synthesis of propolis/$TiO_2$ (P-$TiO_2$) hybrid catalysts

Sol-gel synthesis leads to the excellent distribution of large molecules in ethanolic titanium isopropoxide (TiP) solution and eases the homogenous hydrolysis to produce (P-$TiO_2$) composite. The general procedure is given in Figure 2.

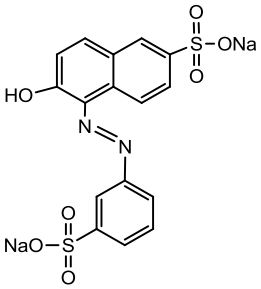


Sunset (SY)

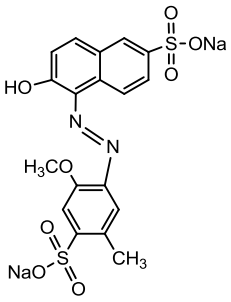


Allura Red (AR)

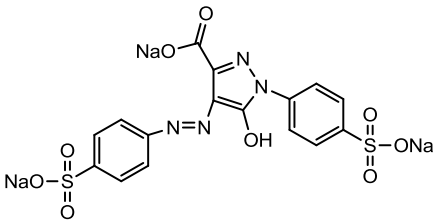


Tartrazine (TT)

**Figure 1.** Chemical structures of each dye molecules.

As given above 8.4 mL of titanium (IV) isopropoxide (TiP) was dissolved in 20 mL absolute ethanol and ethanolic propolis solution was added (0.25, 0.50, 0.75, 1.00 mL). To a solution of acidic ethanol containing 9 mL of absolute ethanol and 1 mL of concentrated $HNO_3$ was added 1 mL of distilled water and slowly added to the first solution before the mixture was left stirring overnight. Then, the mixture was dried at 76°C for 12 h. The obtained powder was calcined for 4 h at 300°C and cooled down to room temperature. The product was kept in dark bottles until use. The same procedure was employed to prepare neat $TiO_2$ powder.

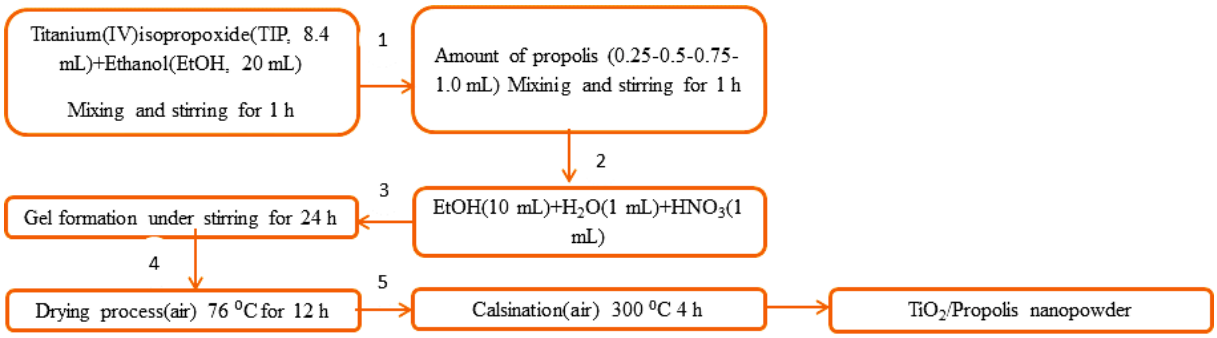


**Figure 2.** General procedure for sol-gel preparation.

### 2.3. Characterization

After preparation and calcination of (P-$TiO_2$) composite the structural properties of solid matter were determined. XRD analysis of the catalysts was carried out by a Rigaku Smartlab diffractometer with CuK$\alpha$ radiation ($\lambda$ = 1.5406 A°) over the range 2$\theta$=20°-60° at room temperature. The surface morphology of the catalysts was determined by SEM analysis (JEOL, JSM 6610). Infrared spectra were obtained with a PerkinElmer 1600 FTIR (4000–400 $cm^{-1}$) spectrometer.

### 2.4. Photocatalytic studies and analysis

Dye solution (100 mL) was placed into photoreactor and hybrid photocatalyst (1.0 g $L^{-1}$) was added to test solution under magnetic stirring. Remaining dye concentration in the presence and absence of light was monitored for 90 and 150 minutes treatment periods.

In the case of photocatalytic experiments, the suspension was illuminated with a UV lamp emitting 254 nm and 365 nm light (6 W, Spectroline ENF-260). Additionally, a LED lamp was used for visible region studies (LED: 300 µW/$cm^2$). A 2.0 mL of the test solution was withdrawn after 150 minutes exposure period. To separate the solid catalyst the sample was centrifuged for 5 min at 3000 rpm by using Eppendorf Centrifuge 5180. The supernatant was used for the determination of the remaining concentration of the dye after filtration with a 0.45 µm membrane filter.

The photodegradation of each dye solution (without catalyst) was also measured. Photocatalytic tests were carried out with neat $TiO_2$ nanoparticles preparing by the same sol-gel procedure. The concentration of each dye was monitored spectrophotometrically at their specific wavelength (Unicam UV-2 spectrometer).

## 3. Results and discussion

### 3.1. Structural analysis of the photocatalysts

$TiO_2$ exists in several polymorphic forms but anatase is being the most active photocatalyst. Sol-gel synthesis and heat treatment at high temperatures dominate the crystal structure [8,9].

Propolis is a heat-sensitive compound and burns out at high-temperature treatment. Calcination at 300°C is a relatively low but enough temperature treatment to obtain anatase structure [10,11]. This temperature is preferred to avoid the thermal degradation of propolis and obtain the desired anatase structure. The XRD pattern of each catalyst is given in Figure 3. The diffraction peak 101 at 2$\theta$=25.50°, originate from anatase $TiO_2$ indicating that the hybrid photocatalysts consist of the pure crystalline anatase phase.

The SEM images are given in Figure 4. The crystalline structure was observed. Smaller nanoparticles distribute over larger crystals due to calcination and aggregation. Small propolis islands are located on larger $TiO_2$ crystals.

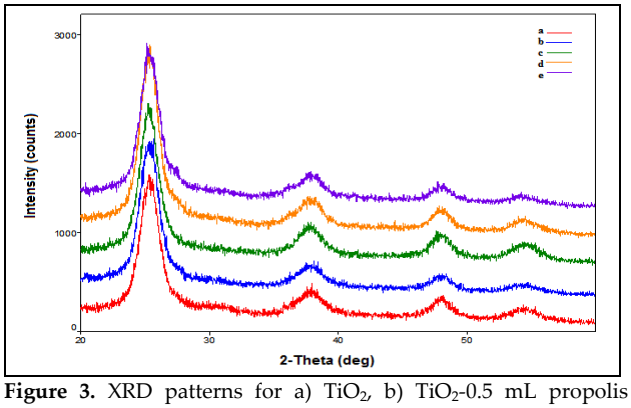


**Figure 3.** XRD patterns for a) $TiO_2$, b) $TiO_2$-0.5 mL propolis solution, c) $TiO_2$-0.25 mL propolis solution, d) $TiO_2$-0.75 mL propolis solution, e) $TiO_2$-1.0 mL propolis solution.

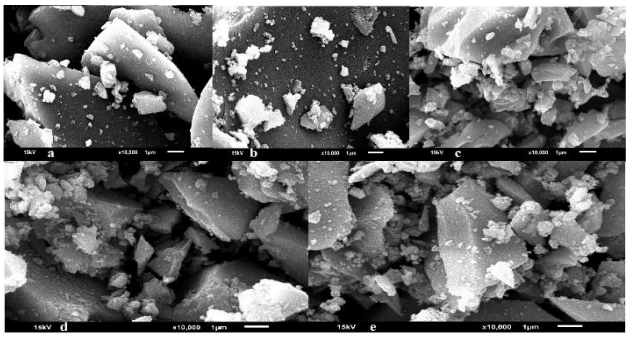

**Figure 4.** SEM image of prepared photocatalysts a) $TiO_2$, b) $TiO_2$-0.5 mL propolis solution, c) $TiO_2$-0.25 mL propolis solution, d) $TiO_2$-0.75 mL propolis solution, e) $TiO_2$-1.0 mL propolis solution.

FTIR spectra of the catalysts are given in Figure 5. Characteristic peaks at 1700-2000 $cm^{-1}$ and 2300-2500 $cm^{-1}$ region belong to propolis doped catalysts represent the organic structure.

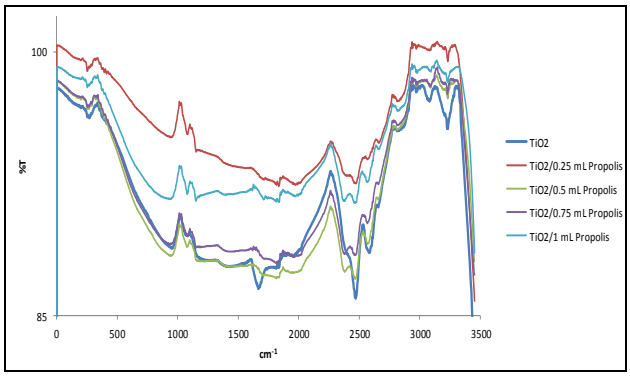


**Figure 5.** FTIR spectra of propolis/$TiO_2$ catalysts.

Propolis contains various organic molecules and the main components are resin (50%-70%), oil and wax (30%-50%), pollen (5%-10%) and other chemical compounds. Additionally, other compounds such as amino acids, minerals, sugars, vitamins B, C and E, flavonoids, phenol are present in this massive structure.

### 3.2. Photocatalytic removal of food dyes

The spectral characters of studied dyes are given in Figure 6. $TiO_2$ itself or propolis doped hybrid catalyst are good adsorbent and can remove pollutants from aqueous medium by using direct adsorption processes. So, the dark adsorption experiments were carried out before photocatalytic treatment.

A set of experiments were designed for dark adsorption measurements and photocatalytic treatments (at λ=254 nm; 365 nm and LED-visible light) were carried out as discussed above. Removal rates are given in Figure 7-9 for each dye.

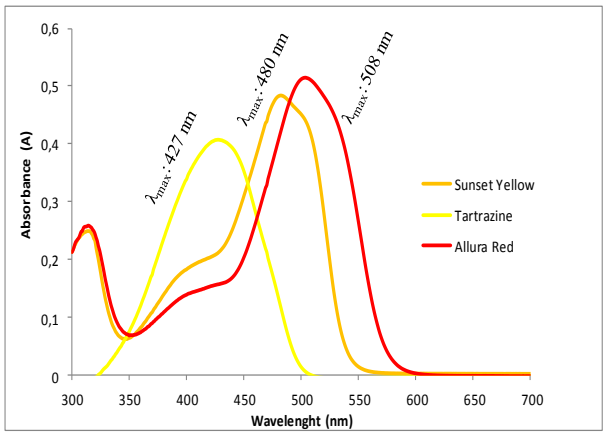


**Figure 6.** UV-vis. spectra of studied food dyes in water ($[C]_0$= 10 mg $L^{-1}$).

Direct adsorption of SY on either neat $TiO_2$ or P-$TiO_2$ was extremely low. However, light exposure for 150 minutes dramatically increased the removal/degradation of SY. As expected, 254 nm light was effective on dye degradation. Neat $TiO_2$ removed 47.07% of SY and SY itself degraded 15.99% without catalyst but with UV light (254 nm). All propolis doped $TiO_2$ catalysts were significantly provided higher removal rates. P-$TiO_2$ produced using 0.75 mL and a 1.00 mL propolis solution was so effective that it removed 91.96% and 86.83%, respectively. It is clear that propolis doping was good strategy for remediation of water contaminated with these dye molecules. More interestingly, 365 nm exposure was effective and 88.01% removal was obtained with P-$TiO_2$ prepared with 1.00 mL propolis solution. This catalyst removed 28.71% of SY concentration after 150 minutes exposure with LED lamp which is producing visible light.

Similar results were obtained for AR dye. Dark adsorption of AR molecules on propolis doped $TiO_2$ catalysts was high (Figure 8). Total removal of the dye was achieved for both 254 nm and 365 nm light exposure after 90 and 150 minutes. Catalysts were able to degrade almost 25% of AR when illuminated with a LED light. Propolis doping resulted in a good catalyst for the effective removal of AR.

Tartrazine (TT) is a common dye for the food industry and has a specific yellow colour. Removal rates are given in Figure 9.

Direct absorption of TT on the catalyst was negligible but photocatalytic removal is quite high for both 254 nm and 365 nm with P-$TiO_2$ 1.00 mL propolis solution. Visible light removal percentages are also significant.

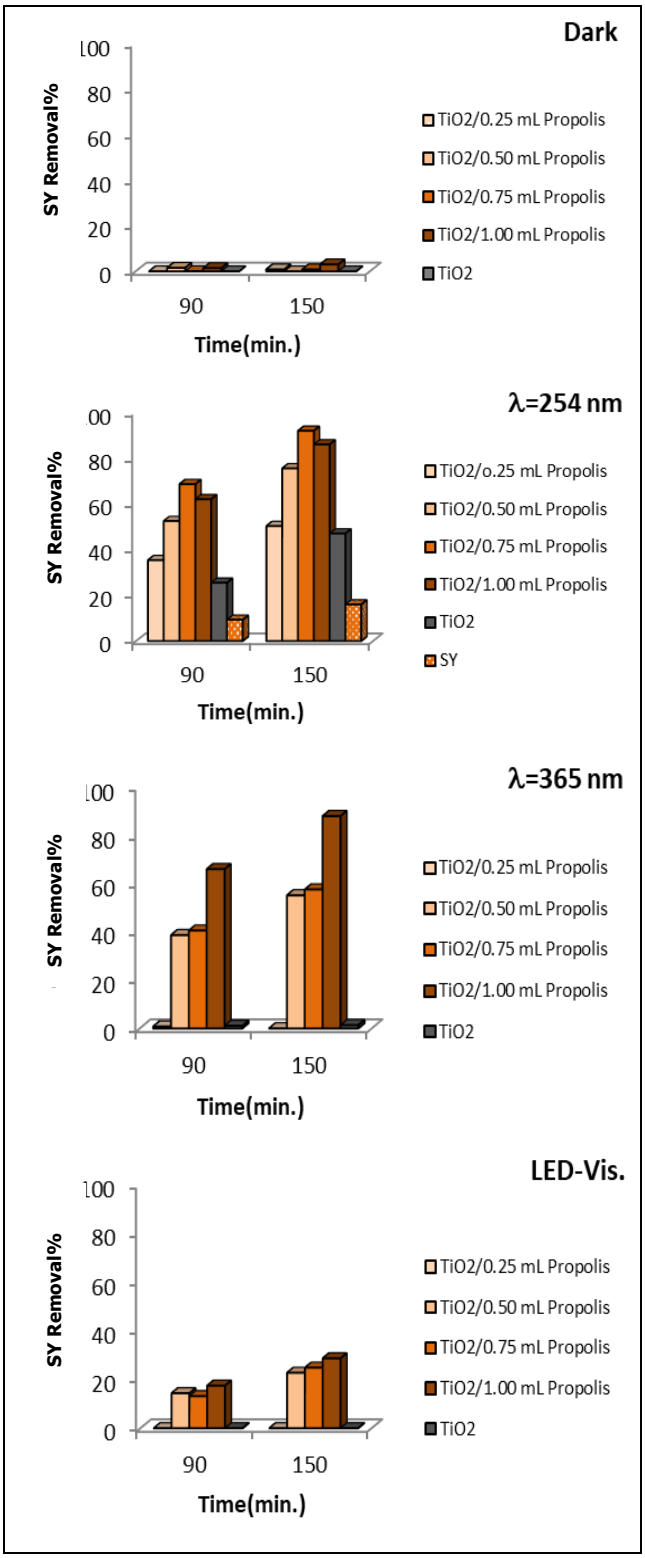


**Figure 7.** The photocatalytic removal of SY ($[C]_0$= 10 mg $L^{-1}$, catalyst mass= 1 g $L^{-1}$, light 254 nm, 365 nm and LED-vis).

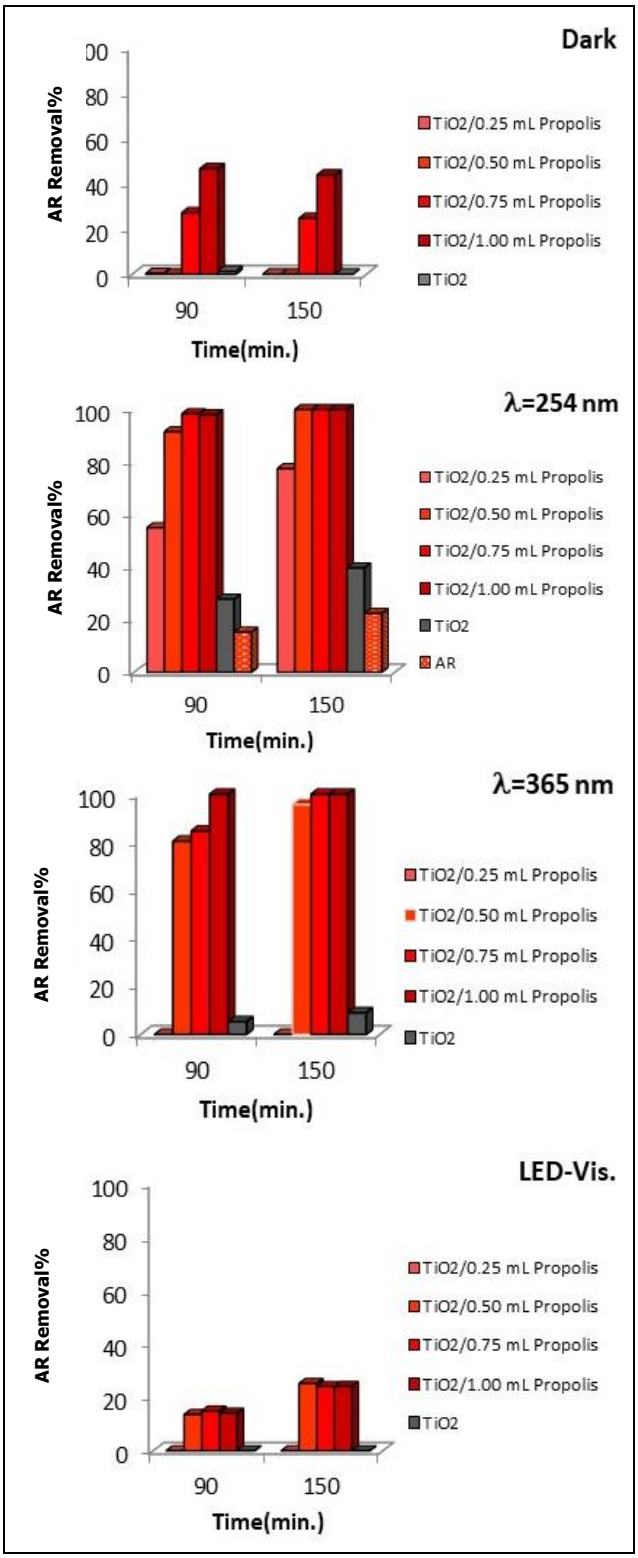


**Figure 8.** The photocatalytic removal of AR ($[C]_0$= 10 mg $L^{-1}$, catalyst mass= 1 g $L^{-1}$, light 254 nm, 365 nm and LED-vis).

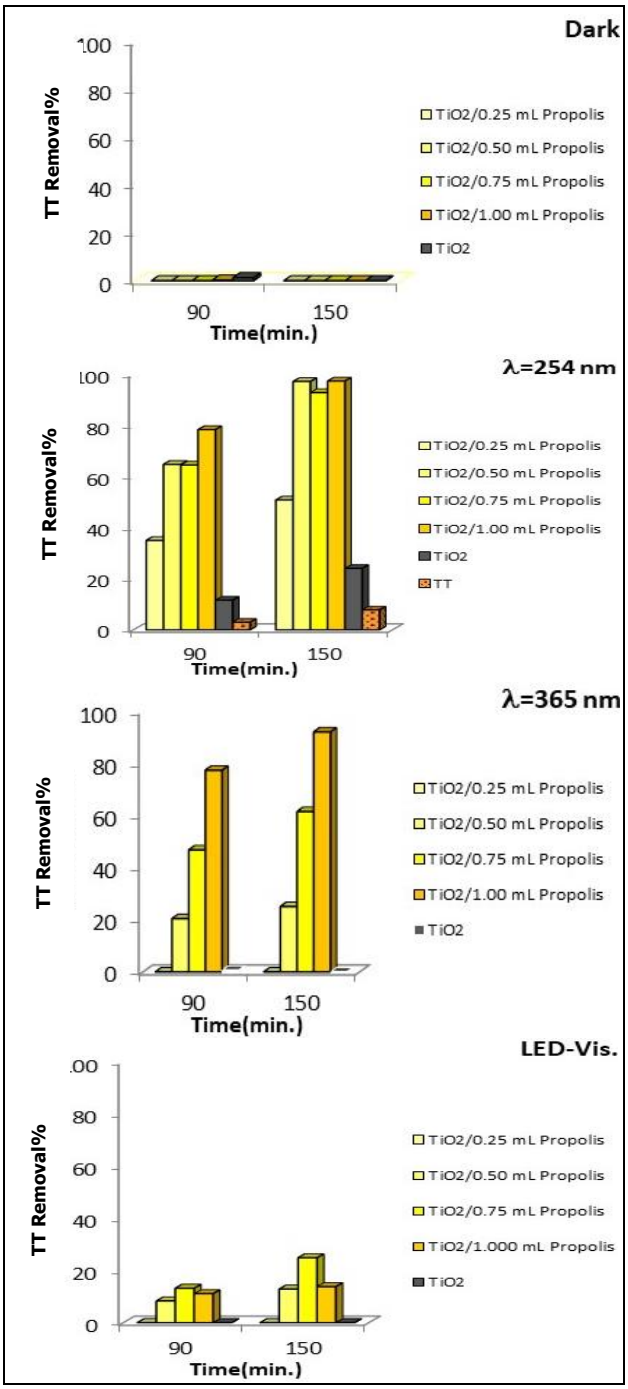


**Figure 9.** The photocatalytic removal of TT ($[C]_0$= 10 mg $L^{-1}$, catalyst mass= 1 g $L^{-1}$, light 254 nm, 365 nm and LED-vis).

## 4. Conclusions

It is shown that propolis doping promotes the electron transfer of titanium dioxide for effective photodegradation of food dye effluents. The catalysts were successfully prepared and characterized the first time and tested for photocatalytic removal of dye pollutants used in the food industry. Catalysts were anatase form and doped propolis amount was quite low. Propolis related carbon doping does not have an enhancing effect on direct absorption of the dye on catalyst but certainly, have an excellent promoting effect on photocatalysis. Surface properties and the form of propolis on the $TiO_2$ surface need more detailed work to explain the mechanistic side of this doping effect.

## Acknowledgments

This work was financially supported by Turkish Research Council (TUBITAK, Grant Number 1649B031600549).

## References

[1] X. Chen, C. Burda, The electronic origin of the visible-light absorption properties of C-, N- and S-doped TiO2 nanomaterials, J Am Chem Soc, 130, 2008, 5018-5019.
[2] A. Zaleska, Doped-$TiO_2$: A review, Recent Pat Eng, 2, 2008. 157-164.
[3] A.C. Martins, A.L. Cazetta, O. Pezoti, J.R.B. Souza, T. Zhang, E. J. Pilau, T. Asefa, V.C. Almeida, Sol-gel synthesis of new $TiO_2$/activated carbon photocatalyst and its application for degradation of tetracycline, Ceram Intern, 43, 2017, 4411-4418.
[4] R. Leary, A. Westwood, Carbonaceous nanomaterials for the enhancement of $TiO_2$ photocatalysis, Carbon, 49, 2011, 741-772.
[5] F. Dong, S. Guo, H. Wang, X. Li, Z. Wu, Enhancement of the visible light photocatalytic activity of C-doped $TiO_2$ nanomaterials prepared by a green synthetic approach, J Phys Chem C 115, 2011, 13285-13292.
[6] M.N.A. Rahman, N.A.A. Rahim, W.F.W. Kamarudin, Z. Irwan, A.R.M. Amin, A. Muhammud, S.M. Muda, N.E.F.M. Akhir, Solar photocatalytic degradation of food dye (Tartrazine) using zinc oxide catalyst, Int J Eng Technol, 7, 2018, 222-226.
[7] M.A. Zazouli, F. Ghanbari, M. Yousefi, S. Madihi-Bidgolie, Photocatalytic degradation of food dye by $Fe_3O_4$-$TiO_2$ nanoparticles in presence of peroxymonosulfate: The effect of UV sources, J Environ Chem Eng, 5, 2017, 2459-2468.
[8] M.R. Ranade, A. Navrotsky, H.Z. Zhang, J.F. Banfield, S.H. Elder, A. Zaban, P.H. Borse, S.K. Kulkarni, G.S. Doran, H.J Whitfield, Energetics of nanocrystalline $TiO_2$, PNAS (99, Suppl 2), 2002, 6476-6481.
[9] H. Zhang, J.F Banfield, Kinetics of crystallization and crystal growth of nanocrystalline anatase in nanometer-sized amorphous titania, J Chem Mater, 14, 2002, 4145-4154.
[10] M. Koç Keşir, G. Dilber, M. Sökmen, M. Durmuş, Use of new quaternized water soluble zinc phthalocyanin derivatives for effective dye sensitization of $TiO_2$, J. Sol-Gel Sci Technol, 2019, https://doi.org/10.1007/s10971-019-05109-w.
[11] M. Sökmen, M. Koc Kesir, S.Y. Alomar, Phthalocyanine-$TiO_2$ nanocomposites for photocatalytic applications: A review, Am J Nanosci, 3, 2017, 63-80.

doi:
e-ISSN: 2687-6698
Research Article
Turkish Journal of Analytical Chemistry
TurkJAC
www.turkjac.org
2019

# HPLC analyses of polyphenolic compounds in oak (*Querces frainetto*) honey from Kırklareli region of Turkey

Yakup Kara[1], Zehra Can[2]*, Sevgi Kolaylı[1]

[1]Karadeniz Technical University, Faculty of Sciences, Department of Chemistry, 61080, Trabzon, Turkey

[2]Bayburt University, Faculty of Applied Sciences, Department of Emergency Aid and Disaster Management, 69000, Bayburt, Turkey

## Abstract

In this study, phenolic profile and total phenolic contents of oak honey, a kind of dark honeydew honey, were determined. The methanolic honey extract was enriched by liquid-liquid extraction with diethyl ether and ethyl acetate, and then was analyzed by RP-HPLC-UV with acetonitrile: water mobile phase. Nineteen phenolic standards were used to prepare calibration graphics. Seven phenolic acid (gallic acid, protocatequic acid, *p*-OH benzoic acid, caffeic acid, syringic acid, *p*-coumaric acid, ferulic acid) and twelve flavonoids (catechin, epicatechin, rutin, myricetin, resveratrol, daidzein, luteolin, *t*-cinnamic acid, hesperetin, chrysin, pinocembrin, caffeic acid phenlyester (CAPE) were used. Total phenolic contents of the honey were measured by Folin Ciocalteau's assay. All of the polyphenols except epicatechin, rutin, luteolin, and hesperetin were detected in varying amounts. Protocatequic acid, ferulic acid, myricetin, and chrysin were the most abundant phenolic compounds. Total phenolic contents of the honey were from 54 to 88 mg GAE/100g. In summary, oak honey has high apitherapeutic value with rich polyphenol diversity.

**Keywords:** Oak honey, antioxidant, phenolic, HPLC, Folin Ciocalteau's

## 1. Introduction

Honey is a natural product and is defined as a functional food. Its composition and biologically active properties depend on the flora and climate of the region where it is produced. According to the sources of production are collected in two classes as blossom and dew honey. Although blossom honey is collected from the flower nectars, dew or secretion honey are made up of different sugar extracts of sweating or insect secretions on trees and leaves [1]. There are two different honeydew honey; one of them is insect secretion honey such as pine honey, and other is a kind of infiltration or percolation some sweet mixtures from leaves, seeds, stems of threes like oak honey [2].

Turkey's seven geographical regions contain many different oak forests, but the Kırklareli region is the most oak honey production area of Turkey. This region has suitable climatic conditions for oak honey production. Oak honey is also known as manna honey and is produced second half of August. In the rainy season, this honey production is reduced. This honey has high viscosity is a dark color, caramelized taste, characteristic smells and non-crystallized. In many studies was determined oak honey has the high antioxidant capacity and that this attribute of polyphenols that contains [2,3]. For the determination of individual phenolic compounds, it is generally necessary their isolation from the sample matrix, then, the identification and the quantification steps. Thus, in this study, we aimed to determine the antioxidant and phenolic profile of oak honey which is rich in polyphenol in the Kırklareli region.

**Citation**: Y. Kara, Z. Can, S. Kolaylı, HPLC analyses of polyphenolic compounds in oak (*querces frainetto*) honey from Kırklareli region of Turkey, Turk J Anal Chem, 1, 2019, 17-20.

***Author of correspondence**: e-mail: zehracan61@gmail.com
Tel: +90 505 8860607
Received: November 12, 2019
Accepted: November 25, 2019

## 2. Experimental

The reagents used were of analytical grade. All phenolic standards were purchased from Merck (Darmstadt, Germany) and Sigma-Aldrich Chemie GmbH (Germany). Folin–Ciocalteu's phenol reagent and TPTZ were obtained from Fluka Chemie GmbH (Switzerland). Trolox was purchased by AppliChem (Darmstadt, Germany).

Iron(III) chlorid hexahydrate ($FeCl_3.6H_2O$), 2,4,6-Tris(2-pyridyl)-s-triazine (TPTZ), iron(II) sulphate heptahydrate ($FeSO_4.7H_2O$), and DPPH (2,2-Diphenyl-1-(2,4,6-trinitrophenyl) hydrazyl) were obtained from Sigma-Aldrich (St. Louis, MO, USA). Glacial acetic acid, sodium acetate, and ferric chloride were supplied from Merck. Sartorius Minisart RC 15 LC syringe filters (RC-membrane, 0.45 μm), Sartorius (Darmstadt, Germany) were employed.

### 2.1. Samples

Six honey samples were obtained from the Kırklareli Beekeepers Union in 2019 and stored at dark room temperature until analysis was performed.

### 2.2. Honey extraction for antioxidant activity and phenolic analysis

Approximately 10 g of each honey was added to an equal volume (50 mL) of 100% methanol and the mixture was continuously stirred with a Heidolph Promax 2020 shaker (Schwabach, Germany) at room temperature for 24 h. Then, particles were removed by using filter paper. The final volume of the obtained solution was set with 100% methanol. The methanolic extract was divided into two parts to make antioxidant tests and phenolic compound analysis.

The methanolic extract was completely evaporated at 40°C using a rotary evaporator. The residue was dissolved in 10 mL of distilled water adjusted to pH 2. Liquid-liquid extraction was applied with 5×3 mL diethyl ether and 5×3 mL ethyl acetate, consecutively [4]. Both diethyl ether and ethyl acetate phases were collected and the solvents were completely removed by rotary evaporation (IKA-Werke, Staufen, Germany) at 40°C. To resuspend the pellet, 2 mL methanol was used.

For HPLC analysis, the suspension was filtered with syringe filters (RC-membrane, 0.45 μm) and injected to the HPLC system.

### 2.3. Total phenolic content (TPC)

The total phenolic content of samples was determined by Folin-Ciocalteu reagent and some modifications were made according to the Slinkard and Singleton methods [5]. Firstly, 400 μL of distilled water of both sample solution and standard solution after, 400 μL of 0.5 N Folin-Ciocalteu reagent was added. After 20 μL sample solution in all samples and 20 μL gallic acid in standard solution was added and then vortexed. After 400 μl of 7.5% of $Na_2CO_3$ was added and then vortexed then incubated for 2 hours at room temperature, absorbance measured at 760 nm using gallic acid as a standard. The results were given as mg gallic acid equivalents per 100 g sample (GAE mg/100g).

### 2.4. Total flavonoid content (TFC)

Total flavonoid content was determined by a colorimetric method as described previously Fukumoto and Mazza [6]. Firstly, 0.25 mL each sample solution, and 2.15 mL methanol 0.05 mL of 10% $Al(NO_3)_3$ and 0.05 mL of 1 M $NH_4CH_3CO_2$ was added to a test tube then was mixed well incubated at room temperature for 40 minutes. Then, the absorbance was measured against the blank 415 nm. The results were expressed as mg quercetin equivalents (QE) per 100 g sample (mg QE/ 100g).

### 2.5. Ferric reducing/antioxidant power (FRAP) assay

The total antioxidant potential of each sample solution was determined using the ferric reducing ability of FRAP assay by Benzie and Strain [7] as a measure of antioxidant power. Briefly, the FRAP reagent was prepared by mixing an acetate buffer (300 μM, pH 3.6), a solution of 10 μM TPTZ in 40 μM HCl, and 20 μM $FeCl_3$. The sample of 50 μL and the FRAP reagent of 1.5 mL were well mixed. The absorbance was taken at 593 nm after 4 min. The standard curve was prepared using different concentrations of $FeSO_4.7H_2O$ and the results were expressed as μmol $FeSO_4.7H_2O$/g).

### 2.6. Analysis of phenolic compounds by HPLC-UV

The samples and standards qualitative analysis and quantitative determination of particular components of the fractions were analysed using high-performance liquid chromatography (HPLC) (Elite LaChrom Hitachi, Japan) with a UV detector. The separation was done on a column with a reversed-

phase C18 column (150 mm×4.6 mm, 5µm; Fortis), in gradient solvent systems A (2% AcOH in water) and solvent B (70:30, acetonitrile/water) which was sonicated before stirring and continuously degassed by the built-in HPLC system. The flow rate was kept constant at 1 mL $min^{-1}$ using gradient programming; starting the flow of mobile phase as B (5%) to three minutes, gradually increasing (up-to 15, 20, 25, 40 and 80% at 8, 10, 18, 25 and 35 minutes respectively) and decreasing to 5 % at 40 minutes and left for 10 minutes to equilibrate in the column. The phenolic profile was determined according to Cakır [8].

## 3. Results and discussion

Flower honey is derived from honeybees are collecting nectar from plants, whereas honeydew is derived from honeybees collected sweet substances mainly from the excretions of plant-sucking insects (Hemiptera) on the living parts of plants or secretions of the living parts of plants.

In this study, was determined antioxidant and phenolic compounds of oak honey are honeydew, honey. Three different methods were utilized to evaluate the antioxidant capacity of the honey; TPC, TFC and the ferric reducing antioxidant assay (FRAP) reflecting total antioxidant capacity. TPC of the kinds of honey varied widely, from 44.75 to 75.58 mg GAE/100 g sample (Table 1).

**Table 1.** Total phenolic, total flavonoid and FRAP of oak honey.

| Samples | TP mg GAE/100 g sample | TF mg QE/100 g sample | FRAP (µmol $FeSO_4.7H_2O$/g sample) |
|---|---|---|---|
| **H1** | 44.75 ± 0.01 | - | 4.16 ± 0.08 |
| **H2** | 54.59 ± 0.02 | 0.06 ± 0.01 | 5.06 ± 0.08 |
| **H3** | 59.30 ± 0.01 | 1.16 ± 0.02 | 4.64 ± 0.06 |
| **H4** | 72.06 ± 0.01 | 1.94 ± 0.04 | 6.40 ± 0.01 |
| **H5** | 75.58 ± 0.01 | 1.99 ± 0.06 | 3.20 ± 0.03 |

TFC of the honey varied widely, from 0.06 to 1.99 mg QE/100 g sample. Frap results of the samples ranged from 3.20 to 6.40 µmol $FeSO_4.7H_2O$/g. Antioxidant compounds in honey samples provided from different climates reflect the floral origin and the biological quality [9]. It is reported that ark amber-colored honey such as oak honeydew honey and chestnut honey have a high antioxidant capacity, resulting from their phenolic compositions [10]. Other studies have also reported that oak honey total phenolic contents of 36.81-62.26 mg GAE/100g [11]. The results are similar to the results of our study. The total polyphenolic content of Anzer honey, light-colored honey, was found 19.50 to-38.30 mg GAE/ 100 g honey in our other studies [12]. According to these results, it was reported that dark honey contains higher phenolic substances and associated antioxidant activity than light-colored honey [11,13,14].

The true quality and, of course, the biological active value of honey is due to the various secondary metabolites present in the structure rather than the sugars it contains [15]. These secondary metabolites have not only anti-oxidant activities, but also anti-microbial, anti-tumoral, and anti-inflammatory functions [11-16].

The phenolic compounds present in the honey were determined by RP-UV-HPLC. In this study, nineteen phenolic standards were used (Figure 1).

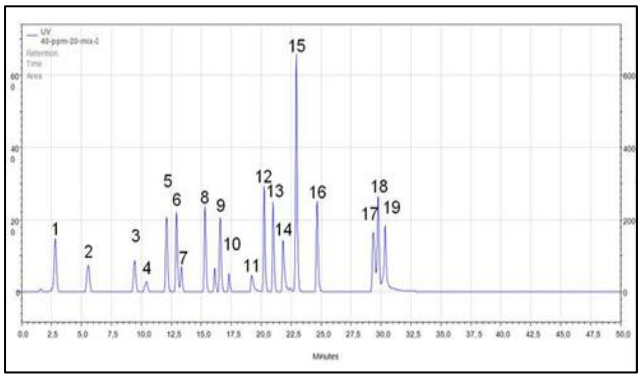


**Figure 1.** HPLC-UV chromatogram of phenolic standards 1. Gallic acid, 2. Protocatequic acid, 3. p-OH Benzoic acid, 4. Catechin, 5. Caffeic acid, 6. Syringic acid, 7. Epicatechin, 8. p-Coumaric acid, 9. Ferulic acid, 10. Rutin, 11. Myricetin, 12. Resveratrol,13. Daidzein, 14. Luteolin, 15. t-Cinnamic acid, 16. Hesperidin, 17. Chrysin, 18. Pinocembrin, 19. CAPE

The phenolic component results of honey are as in Table 2. All standards except for luteolin, epicatechin and hesperidin were detected at different concentrations. Our previous study determined that catechin, vanillic acid, syringic acid, daidzein, and luteolin were not detected in any specimens [3].

In this study was not detected luteolin in any honey. In our findings, protocatechuic acid, ferulic acid, myricetin, and chrysin have been reported as major phenolic compounds in oak honey. In our previous study was found protocatechuic and ferulic acid as major phenolic compounds in oak honey [3].

**Table 2.** Phenolic profiles of the oak honeys.

| Standards | H1 | H2 | H3 | H4 | H5 |
|---|---|---|---|---|---|
| | (μg extract/g sample) | | | | |
| Gallic acid | 1.04 | 1.85 | 1.55 | 3.33 | 0.34 |
| Protocateuic acid | 5.07 | 8.20 | 12.74 | 14.83 | 5.64 |
| *p*-OH Benzoic acid | 2.70 | 2.02 | 0.89 | 1.32 | 4.69 |
| Catechin | 0.89 | n.d. | n.d. | n.d. | 1.28 |
| Caffeic acid | 0.92 | 0.49 | 0.77 | 0.98 | 1.84 |
| Syringic acid | 0.59 | 0.26 | 0.53 | 0.67 | 1.36 |
| Epicatechin | n.d. | n.d. | n.d. | n.d. | n.d. |
| *p*-Coumaric acid | 0.63 | 0.86 | 0.48 | 0.62 | 1.50 |
| Ferulic acid | 1.75 | 4.89 | 2.96 | 5.03 | 0.39 |
| Rutin | n.d. | n.d. | n.d. | n.d. | 6.47 |
| Myricetin | 7.42 | 4.33 | 3.70 | 3.10 | 9.89 |
| Resveratrol | 1.25 | 0.56 | 0.61 | 0.76 | 0.79 |
| Daidzein | 2.04 | 0.87 | 0.75 | 0.98 | 2.16 |
| Luteolin | n.d. | n.d. | n.d. | n.d. | n.d. |
| *t*-Cinnamic acid | 0.02 | 0.09 | 0.21 | 0.42 | 0.11 |
| Hesperidin | n.d. | n.d. | n.d. | n.d. | n.d. |
| Chrysin | 2.68 | 1.70 | 2.28 | 2.81 | 3.32 |
| Pinocembrin | 2.00 | 0.28 | 1.21 | 1.81 | 2.94 |
| CAPE | 0.68 | 0.24 | 0.33 | 0.74 | 1.30 |

n.d.: not detected

Oak honey samples provided from the same botanical origins and biogeographical areas of production were analyzed. In this study, 5 oak honey samples collected from the Thrace region of Turkey exhibited honeydew honey characteristics, depending on their antioxidant activities and phenolic profiles. The oak honey had higher antioxidant activity and most phenolic compounds than light-colored honey. It is expected that the results will contribute to a more accurate evaluation of oak honey in the literature.

## References


[1] S. Simova, A. Atanassov, M. Shishiniova, V. Bankova, A rapid differentiation between oak honeydew honey and nectar and other honeydew honeys by NMR spectroscopy, Food Chem, 134(3), 2012, 1706-1710.

[2] A. Ozkok, K. Sorkun, Some characteristic features of oak (quercus frainetto ten.) Fresenius Environ Bull, 27, 2018, 8359-8366.

[3] S. Kolayli, Z. Can, H. E. Çakir, O. T. Okan, O. Yildiz, An investigation on Trakya region oak (Quercus spp.) honeys of Turkey: Their physico-chemical, antioxidant and phenolic compounds properties, Turk J Biochem, 43(4), 2018, 362-374.

[4] K.H. Kim, R. Tsao, R. Yang, S.W. Cui, Phenolic acid profiles and antioxidant activities of wheat bran extracts and the effect of hydrolysis conditions, Food Chem, 95(3) 2006, 466-473.

[5] K. Slinkard, V.L. Singleton, Total phenol analyses: Automation and comparison with manual methods, Am J Enol Viticult, 28, 1977, 49-55.

[6] L.R. Fukumoto, G. Mazza, Assessing antioxidant and prooxidant activities of phenoliccompounds, J Agr Food Chem, 48, 2000, 3597-3604.

[7] I.F.F. Benzie, J.J. Strain, Ferric reducing/antioxidant power assay: Direct measure of total antioxidant activity of biological fluids and modified version for simultaneous measurement of total antioxidant power and ascorbic acid concentration, Method Enzymol, 299, 1999, 15-27.

[8] H.E. Çakır, Y. Şirin, S. Kolaylı, Z. Can, Validation methods for phenolic components with RP-HPLC-UV in various bee products, Apiterapi ve Doğa Dergisi, 1(1), 2018, 13-19.

[9] O. Muñoz, S. Copaja, H. Speisky, R.C. Peña, G. Montenegro, Contenido de flavonoides ycompuestos fenólicos de mieles chilenas e índice antioxidante, Quim. Nova, 30, 2007, 848-851.

[10] [9] M. C. Seijo, O. Escuredo, M. S. Rodríguez-Flores, Physicochemical properties and pollen profile of oak honeydew and evergreen oak honeydew honeys from Spain: A comparative study, Foods, 8(4), 2019, 126.

[11] H. Sahin, Honey as an apitherapic product: its inhibitory effect on urease and xanthine oxidase, J Enzyme Inhib Med Chem, 31(3), 2016, 490-494.

[12] M. Malkoç, H.E. Çakır, Y. Kara, Z. Can, S. Kolaylı, Phenolic composition and antioxidant properties of Anzer honey from black sea region of Turkey, Uludag Arıcılık Dergisi, doi.org/10.31467/uluarıcılık. 2019, 602906.

[13] [12] A.M. González-Paramás, R.J. García-Villanova, J.A.G. Bárez, J. S. Sánchez, R. A. Albajar, Botanical origin of monovarietal dark honeys (from heather, holm oak, pyrenean oak and sweet chestnut) based on their chromatic characters and amino acid profiles, Eur Food Res Technol, 226(1-2), 2007, 87-92.

[14] Z. Can, O. Yildiz, H. Sahin, E.A. Turumtay, S. Silici, S. Kolayli, An investigation of Turkish honeys: Their physico-chemical properties, antioxidant capacities and phenolic profiles, Food Chem, 180, 2015, 133-141.

[15] M. Malkoç, Y. Kara, A. Özkök, Ö. Ertürk, S. Kolaylı, Karaçalı (*Paliurus spina-christi* Mill.) balının karakteristik özellikleri, Uludag Arıcılık Dergisi. 19(1), 2019, 69-81.

[16] O. Yıldız, Z. Can, Ö. Saral, E. Yuluğ, F. Öztürk, R. Aliyazıcıoğlu, S. Kolaylı, Hepatoprotective potential of chestnut bee pollen on carbon tetrachloride-induced hepatic damages in rats, Evid-Based Complementary Altern Med, 2013, 461478.

doi:
e-ISSN: 2687-6698
Research Article

Turkish Journal of Analytical Chemistry
www.turkjac.org
2019
TurkJAC

# A novel silicone phthalocyanine for the preconcentration and spectrophotometric determination of copper by ionic liquid-based dispersive liquid-liquid microextraction

Yasemin Çağlar[1]*, Ece Tuğba Saka[2]

[1]Giresun University, Faculty of Engineering, Department of Genetic and Bioengineering, 28200, Giresun, Turkey
[2]Karadeniz Technical University, Faculty of Science, Department of Chemistry, 61080, Trabzon, Turkey

## Abstract

Dispersive liquid-liquid microextraction (DLLME) is of interest as an environmentally friendly sample preparation technique due to its simplicity, operating speed and low solvent and reagent consumption. Accordingly, this work reports the development of a new simple ionic liquid-based dispersive liquid-liquid microextraction (IL-DLLME) method for spectrophotometric copper determination. First, the copper was complexed with a novel silicone phthalocyanine and then the complex was extracted into 1-heptyl-3-methylimidazolium hexafluorophosphate dissolving in acetone in the presence of sodium dodecyl sulfate (SDS) as the anti-sticking agent. After centrifuging for 2 min at 3000 rpm, the extracting phase was diluted to 250 μL with acetone for spectrophotometric detection at 340 nm. Some experimental conditions that influence the procedure were optimized. The pH and complexing reagent concentration are 4.0 and $4.6\times10^{-6}$ mol/L, respectively. The method is linear in the range from 0.03 to 100 μg/mL with a correlation coefficient ($R^2$) of 0.9973. The limit of detection (LOD) of the method is 17 μg/L. The relative standard deviation is 1.7% at 45 μg/mL $Cu^{2+}$ (n=6). The enrichment factor for the method was calculated as 210.

**Keywords:** Dispersive liquid-liquid microextraction, silicone phthalocyanine, Cu preconcentration, ionic liquids, spectrophotometry

## 1. Introduction

Most of the scientists who have been researching analytical chemistry for the last ten years have adopted green chemistry and have turned to extraction methods in which fewer solvents were used. This technique is dispersive liquid-liquid microextraction (DLLME) tendering high diversification factors from low volumes of different samples. Its simplicity, low cost, and ease of method development make this technique feasible to virtually all analytical laboratories. [1]. This technique was first applied by Rezaee in 2006 for organic analytes. It has become an increasingly popular technique, not only in chemistry and biochemistry but also in genetic and molecular biology, chemical engineering, environmental science, medicine, engineering, agriculture and biological sciences, pharmacology, toxicology and pharmacy, social sciences and others [2-3].

Phthalocyanine compounds to which different groups can be easily bound have significant absorbances in the 600-800 nm range. Thanks to the 18-π electron system of the phthalocyanine ring, it is a good electron donor (e-donor) molecule and has excellent photo-sensitizing properties. Silicone phthalocyanines (SiPc) have received more attention from researchers in the last decade, due to their thermal, chemical stability and bright blue-green colors [4-6]. They were used for PDT application [7-9], dye-sensitized solar cells [10-11], fluorescence sensors [12-13], fluorophores [14-15], and optical, electronic and photo-electronic devices [16-17].

**Citation**: Y. Çağlar, E.T. Saka, A novel silicone phthalocyanine for the preconcentration and spectrophotometric determination of copper by ionic liquid-based dispersive liquid-liquid microextraction, Turk J Anal Chem, 1, 2019, 21-25.

***Author of correspondence**: e-mail: go_yasemin@hotmail.com
Tel.: +90 454 3104016, Fax: +90 454 3101749
Received: October 16, 2019
Accepted: November 06, 2019

Copper is a trace element that shows a significant role in many biochemical reactions such as hemoglobin synthesis, the usual task of the central nervous system and oxidative phosphorylation [18-19]. For many living organisms, a daily intake of Cu is 0.5 mg/L [20]. If this limit is exceeded, the neurological ailments such as schizophrenia, depression, epilepsy [21] and irritation of nose and throat, nausea, vomiting, and diarrhea will disappear [22]. Some methods to determination of Cu(II) from various samples are liquid-liquid extraction [23], solid phase extraction (SPE) [24] and cloud point extraction (CPE) [25]. Today, microextraction methods placed for minifying organic solvent consumption, facilitating sample preparation steps, providing high enrichment rates and appropriate to automation [26].

In this work, IL-DLLME is used for the determination of Cu(II) with silicone phthalocyanine as an interaction agent. This developed method includes the extraction of Cu(II) in the ionic liquid droplets after interact with silicone phthalocyanine compound (Figure 1).

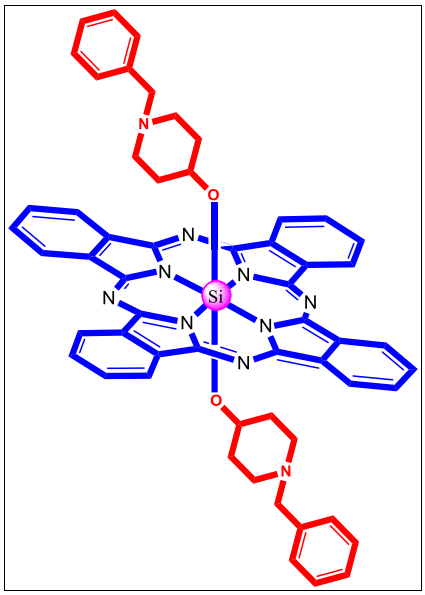


**Figure 1.** The structure of silicone phthalocyanine.

## 2. Experimental

### 2.1. Reagents and apparatus

All the reagents and apparatus that used were given in the supplementary material file.

## 3. Results and discussion

### 3.1. Optimization of IL-DLLME procedure

*3.1.1. Selection of IL*

In this study, we used ionic liquids as extraction solvent. The selected ionic liquids should be hydrophobic and have high extraction ability of the target molecules. 1-hexyl-3-methylimidazolium hexafluorophosphate ([C6-mim][$PF_6$]), 1- butyl-3-methylimidazolium hexafluorophosphate ([C4-mim][$PF_6$]), 1-methyl-3-octylimidazolium hexafluorophosphate ([C8-mim][$PF_6$]), 1-heptyl-3-methylimidazolium hexafluorophosphate ([C7-mim][$PF_6$]), and 1-butyl-3-pentylimidazolium hexafluorophosphate ([C4-C5im][PF6]) were studied as extracting solvents using 1000 mL of acetone as disperser solvent.

According to the results, 1-heptyl-3-methylimidazolium hexafluorophosphate was opted as the extraction solvent for further experiments (Fig. 2).

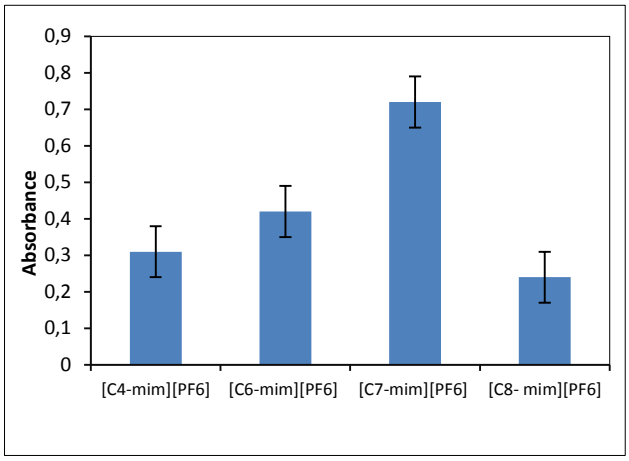


**Figure 2.** Effect of IL. Conditions: sample volume 15 mL, pH=4.0, disperser solvent (acetone) 1000 mL, silicone phthalocyanine $4.6\times10^{-5}$ mol/L, centrifugation 2 min at 3000 rpm. The error bar is the standard deviation (n=3).

*3.1.2. Selection of the disperser solvent*

In DLLME that is a three-component solvent system, the disperser solvent has to be miscible with both water and ionic liquid [27, 28]. Acetone, acetonitrile, ethanol, and methanol as the commonly used disperser solvent were examined. When the results were evaluated, it was decided that acetone was the most suitable dispersion solvent (Fig 3).

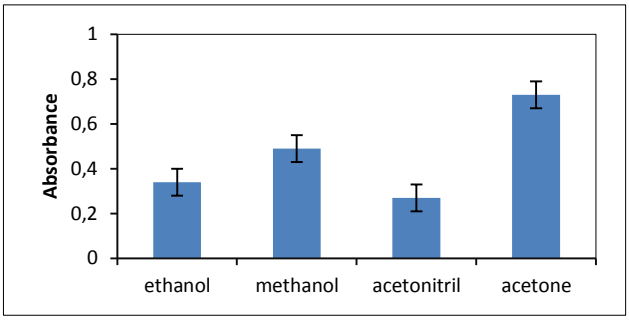


**Figure 3**. Effect of disperser solvent. Conditions: sample volume 15 mL, pH=4.0, extractive solvent (IL) 300 µL, silicone phthalocyanine $4.6\times10^{-5}$ mol/L, centrifugation 2 min at 3000 rpm. The error bar is the standard deviation (n=3).

### 3.1.3. *Effect of the IL volume*

Different volumes (50, 100, 150, 200, 250, 300, 350 and 400 µL) of 1-heptyl-3-methylimidazolium hexafluorophosphate was tested to ensure maximum extraction efficiency in the proposed DLLME procedure. The results showed that the extraction efficiency increased with the increasing volume of 1-heptyl-3-methylimidazolium hexafluorophosphate from 50 to 300 µL, and then decreased. 300 µL was selected as an optimum volume of extracting solvent.

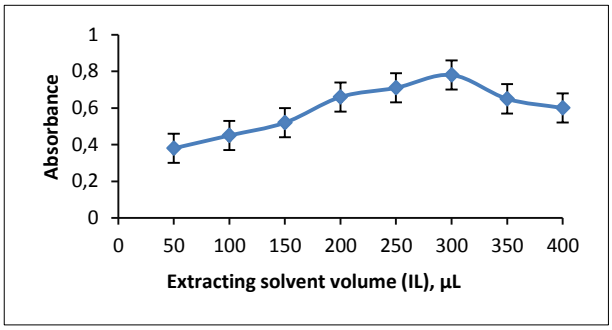


**Figure 4.** Effect of IL volume. Conditions: sample volume 15 mL, pH=4.0, disperser solvent (acetone) 1000 mL, silicone phthalocyanine $4.6\times10^{-5}$ mol/L, centrifugation 2 min at 3000 rpm. The error bar is the standard deviation (n=3).

### 3.1.4. *Effect of the disperser solvent volume*

The disperser solvent volume has quite influence in DLLME procedure because affects the dispersion of the extraction solvent in aqueous analyte phase. In the range of 400 to 1200 mL of acetone containing 300 µL of 1-heptyl-3-methylimidazolium hexafluorophosphate was researched to specify ideal disperser solvent volume. Considering the results 1000 mL of acetone was chosen as an ideal disperser solvent volume in the microextraction procedure (Fig. 5).

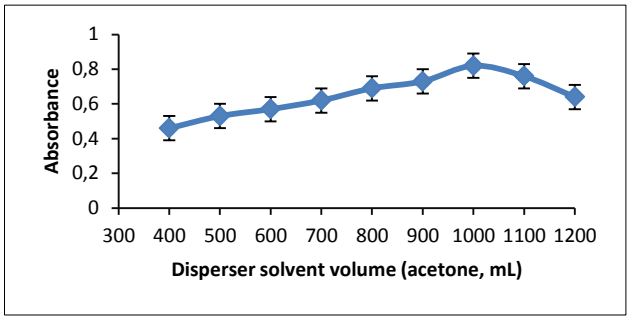


**Figure 5**. Effect of disperser solvent volume. Conditions: sample volume 15 mL, pH=4.0, extracting solvent (IL) 300 µL, silicone phthalocyanine $4.6\times10^{-5}$ mol/L, centrifugation 2 min at 3000 rpm. The error bar is the standard deviation (n=3).

### 3.1.5. *Effect of pH*

Determination of the optimum pH in the DLLME procedure is an important step because pH influences the chelation of Cu(II)-silicone phthalocyanine and subsequent extraction into the IL phase. Various sample solutions ranging from pH 1-10 were prepared and extraction efficiencies were examined. The experimental results are spotted in Fig. 6. The highest extraction yield of Cu(II)-silicone phthalocyanine into the ionic liquid was obtained at pH 4.0. The absorbance increased when the pH of the sample solution increased from 2.0 to 4.0. After pH 4.0, absorbance began to decrease. In the pH range of 8-10, absorbance leveled off.

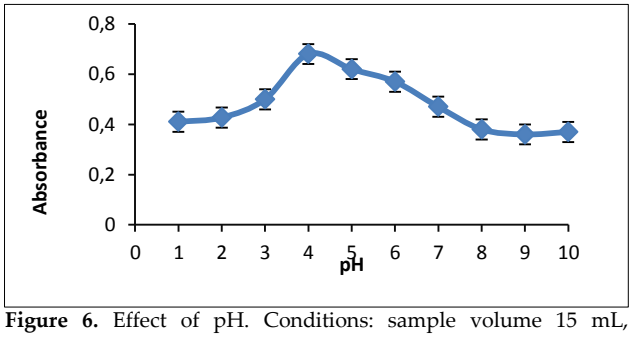


**Figure 6.** Effect of pH. Conditions: sample volume 15 mL, extracting solvent volume (IL) 300 µL, disperser solvent (acetone) 1000 mL, silicone phthalocyanine $4.6\times10^{-5}$ mol/L, centrifugation 2 min at 3000 rpm. The error bar is the standard deviation (n=3).

### 3.1.6. *The concentration of silicone phthalocyanine*

The silicone phthalocyanine concentration directly affects the complexation of Cu(II). Sample solutions containing various concentrations ($1\times10^{-4}$-$1\times10^{-6}$ mol/L) of silicon phthalocyanine were prepared and the proposed microextraction procedure was applied to these solutions. It was found that the absorbance signal of the Cu(II) complex increased by increasing the silicon phthalocyanine concentration up to $4.6\times10^{-5}$ mol/L and then it remained fixed. So,

$4.6\times10^{-5}$ mol/L was assigned as working concentration.

*3.1.7. Selection of the anti-sticking agent*

The loss of some extraction phase in the centrifugation step when ionic liquid is used in the DLLME procedure is an important problem that must be overcome. The addition of a surfactant to the sample solution is often used to solve this problem. Drops of ionic liquid are surrounded by surfactant molecules and their interaction with the test tube is reduced [29]. We also investigated the effect of some surfactants such as SDS, Triton X-100 and Triton X-114 on increasing extraction efficiency. The results showed that these 3 surfactants were effective in preventing sticking but the best yield was obtained with SDS.

### 3.2. Interferences

The potential interference effects of various cations ($Co^{2+}$, $Ni^{2+}$, $Zn^{2+}$, $Ag^{+}$, $Cr^{3+}$, $Mn^{2+}$, $Fe^{3+}$) and anions ($NO_3^-$, $SO_4^{2-}$, $PO_4^{3-}$) on the proposed method were investigated. For this purpose, the absorbance values of the solutions with and without foreign ions at 340 nm were compared. The concentration of foreign ions that did not cause a difference of more than 5% was determined as the tolerance limit. In this step, a 10 ml sample solution of 0.1 μg/mL Cu(II) was used. The results are given in Table 1. The results show that the proposed ionic liquid-based DLLME method for spectrophotometric Cu(II) determination is highly selective.

**Table 1.** Tolerance limits of coexisting ions.

| Ion | Tolerance limits μg/mL |
|---|---|
| $Co^{2+}$ | 438 |
| $Ni^{2+}$ | 491 |
| $Zn^{2+}$ | 523 |
| $Ag^{+}$ | 675 |
| $Cr^{3+}$ | 389 |
| $Mn^{2+}$ | 210 |
| $Fe^{3+}$ | 660 |
| $NO_3^-$ | 790 |
| $SO_4^{2-}$ | 809 |
| $PO_4^{3-}$ | 205 |

### 3.3. Analytical characteristic

The proposed DLLME method was validated using 10 ml of standard Cu(II) solution under optimum conditions. Some basic parameters such as linear range, correlation coefficient ($R^2$), limit of detection (LOD), limit of quantification (LOQ), relative standard deviation (RSD) and enrichment factor (EF) were examined for validation. The data obtained are remarked in Table 2. A linear increase between the absorbances and the concentrations of Cu(II) in the range of 0.03-100 μg/mL was observed. The correlation coefficient was 0.9973. The LOD was 17 μg/L based on three times Sd/m ratio and The LOQ was 42 μg/L based on nine times Sd/m ratio, where the Sd was the standard deviation of eleven blank and m was the slope of the calibration graph. The EF was calculated as 210 using the ratio of analyte concentrations in the ionic phase and initial aqueous phase. The RSD for 45 μg/mL of Cu(II) was 1.7% (n=6).

**Table 2.** Analytical features of proposed method under optimum conditions.

| | |
|---|---|
| Correlation coefficient ($R^2$) | 0.9973 |
| Linear range (μg/mL) | 0.03-100 |
| LOD (μg/L) | 17 |
| LOQ (μg/L) | 42 |
| RSD, %(n=6) | 1.7 |
| Enrichment factor | 210 |

## 4. Conclusion

The selective determination of metal ions in environmental samples has been a subject of considerable interest. Despite significant advances in technology, few techniques allow direct determination from sample matrix [30]. Thus, a pre-concentration step is often required. DLLME is an effective pre-concentration method that is widely used nowadays.

In this study, a novel DLLME method was developed for the spectrophotometric determination of Cu (II). The method is simple, fast, selective and inexpensive. Furthermore, since we use an ionic liquid as an extraction solvent, it is very environmentally friendly. Ionic liquids are good alternatives to conventional organic solvents because of their low vapor pressure, high thermal stability, wide liquid range, relatively high viscosity, and especially low toxicity. They are widely recognized as so-called green solvents. When the method performance is evaluated, the proposed method seems to be very suitable for the determination of Cu in environmental samples.

## References


[1] A. Spietelun, L. Marcinkowski, M. Guardia, J. Namieśnik, Green aspects, developments and perspectives of liquid phase microextraction techniques, Talanta, 119, 2014, 34-45.

[2] M. Rezaee, Y. Assadi, M.R. Milani Hosseini, E. Aghaee, F. Ahmadi, S. Berijani, S. Determination of organic compounds in water using dispersive liquid-liquid microextraction, J Chromatogr A, 1116, 2006, 1-9.

[3] A.V. Herrera-Herrera, M. Asensio-Ramos, J. Hernàndez-Borges, M.A. Rodriguez Delgado, Dispersive liquid-liquid microextraction for determination of organic analytes, Trends Anal Chem 29 (7), 2010, 728-751.

[4] K.M. Kadish, K.M. Smith, R. Guilard, Handbook of porphyrin science, Singapore: World Scientific Publishing, 2010.

[5] M.P. Donzello, C. Ercolani, V. Novakova, P. Zimcik, P.A. Stuzhin, Tetrapyrazinoporphyrazines and their metal derivatives. Part I: Synthesis and basic structural information, Coord Chem Rev 309, 2016, 107-179.

[6] M.P. Donzello, D. Vittori, E. Viola, L.H. Zeng, Y. Cui, K.M. Kadish, Tetra-2,3-pyrazinoporphyrazines with externally appended pyridine rings 14: UV-visible spectral and electrochemical behavior of homo/heterobinuclear neutral and hexacationic macrocycles, J Porphyr Phthalocyanines, 17, 2015, 896-904.

[7] M. Kucinska, P. Skupin-Mrugalska, W. Szczolko, L. Sobotta, M. Sciepura, E. Tykarska, Phthalocyanine derivatives possessing 2-(morpholin-4-yl)ethoxy groups as potential agents for photodynamic therapy, J Med Chem, 58, 2015, 2240-2255.

[8] M. Wang, L. Huang, S.K Sharma, S. Jeon, S. Thota, F.F. Sperandio, S. Nayka, J. Chang, M.R. Hamblin, L.Y. Chiang, Synthesis and photodynamic effect of new highly photostable decacationically armed [60]- and [70]fullerene decaiodide monoadducts to target pathogenic bacteria and cancer cells, J Med Chem, 55, 2012, 4274-4285.

[9] M.P. Donzello, E. Viola, C. Ercolani, Z. Fu, D. Futur, K.M. Kadish, Tetra-2,3-pyrazinoporphyrazines with externally appended pyridine rings. 12. New heteropentanuclear complexes carrying four exocyclic cis-platin-like functionalities as potential bimodal (PDT/cis-platin) anticancer agents, Inorg Chem, 51, 2012, 12548-12559.

[10] A. Hagfeldt, G. Boschloo, L.C. Sun, L. Kloo, H. Pettersson, Dye-sensitized solar cells, Chem Rev 110, 2010, 6595-6663.

[11] M-E Ragoussi, M. Ince, T. Torres, Recent advances in phthalocyanine based sensitizers for dye sensitized solar cells, Eur J Org Chem 29, 2013, 6475-6489.

[12] L. Lochman, J. Svec, J. Roh, K. Kirakci, K. Lang, P. Zimcik, Azaphthalocyanines: Red fluorescent probes for cations, Chem Eur J, 22, 2016, 2417-2426.

[13] V. Novakova, M. Laskova, H. Vavrickova, P. Zimcik, phenol substituted tetrapyrazinoporphyrazines: pH dependent fluorescence in basic media, Chem Eur J, 21, 2015, 14382-14392.

[14] I.V. Nesterova, C.A. Bennett, S.S. Erdem, R.P. Hammer, P.L. Deininger, S.A. Soper, Near-IR single fluorophore quenching system based on phthalocyanine (Pc) aggregation and its application for monitoring inhibitor/activator action on a therapeutic target: L1-EN, Analyst, 136, 2011, 1103-1105.

[15] P. Zimcik, V. Novakova, K. Kopecky, M. Miletin, R.Z. Uslu Kobak, E. Svandrlikova, Magnesium azaphthalocyanines: An emerging family of excellent red-emitting fluorophores, Inorg Chem, 51, 2012, 4215-4223.

[16] D. Wohrle, G. Schnurpfeil, S.G. Makarov, A. Kazarin, O.N. Suvorova, Practical applications of phthalocyanines – from dyes and pigments to materials for optical, electronic and photo-electronic devices, Macroheterocycles, 5, 2012, 191-202.

[17] P. Zimcik, A. Malkova, L. Hruba, M. Miletin, V. Novakova, Bulky 2,6-diphenylphenylsulfanyl substituents efficiently inhibit aggregation in phthalocyanines and tetrapyrazinoporphyrazines and control their photophysical and electrochemical properties, Dyes Pigm 136, 2017, 715-723.

[18] T.W. Lin, S.D. Huang, Direct and simultaneous determination of copper, chromium, aluminum and manganese in urine with a multielement graphite furnace atomic absorption spectrometer, Anal Chem, 73 (17), 2001, 4319-4325.

[19] C.N. Sawyer, P.L. McCarty, G.F. Parkin, Chemistry for Environmental Engineering, fourth ed., McGraw-Hill, New York, 1996, p. 634.

[20] L. Feng, Y. Zhang, L. Wen, Z. Shen, Y. Guan, Colorimetric determination of copper (II) ions by filtration on sol-gel membrane doped with diphenylcarbazide, Talanta, 84 (3), 2011, 913-917.

[21] C. Pfeiffer, R. Mailloux, Excess copper as a factor in human diseases, J Orthomol Med, 2 (3), 1987, 171-182.

[22] Y. Yamini, J. Hassan, M.H. Karbasi, Solid phase extraction of copper and cupron on octadecyl silica cartridge and its determination with atomic absorption spectrometry, Microchim Acta 148 (3-4), 2004, 305-309.

[23] D. Alkan, M. Kara, Preconcentration and separation of copper (II) with solvent extraction using N,N′-bis(2-hydroxy-5-bromo-benzyl)1,2 diaminopropane, Microchem J, 71, 2002, 29-39.

[24] A. Tobiasz, S. Walas, A. Soto Hernandes, H. Mrowiec, Application of multiwall carbon nanotubes impregnated with 5- dodecylsalicylaldoxime for on-line copper preconcentration and determination in water samples by flame atomic absorption spectrometry, Talanta, 96, 2012, 89-95.

[25] Y. Gao, P. Wu, W. Li, Y. Xuan, X. Hou, Simultaneous and selective preconcentration of trace Cu and Ag by one-step displacement cloud point extraction for FAAS determination, Talanta 81, 2010, 586-590.

[26] E. Alver, A. Demirci, M. Ozcimder, Microextraction methods, Sigma J Eng Nat Sci 30, 2012, 75-90.

[27] G. Kandhro, M. Soylak, T.G. Kazı, E. Yılmaz, Enrichment of copper as 1-(2-pyridylazo)-2-naphthol complex by the combination of dispersive liquid-liquid micro-extraction/flame atomic absorption spectrometry, J AOAC Int 97, 2014, 205-210.

[28] E. Stanisz, A. Zgola-Grzeskowiak, In situ metathesis ionic liquid formation dispersive liquid-liquid microextraction for copper in water samples by electrothermal atomic absorption spectrometry, Talanta, 115, 2013, 178-183.

[29] M. Baghdadi, F. Shemirani, Cold-induced aggregation microextraction: A novel sample preparation technique based on ionic liquids, Anal Chim Acta, 613, 2008, 56-63.

[30] Y. Çağlar, E.T. Saka, H. Alp, H. Kantekin, Ü. Ocak, M. Ocak, A Simple spectrofluorimetric method based on quenching of a nickel(II)-phthalocyanine complex to determine iron (III), J Fluorescence, 26, 2016, 1381-1389.